



上海交通大学学位论文

海铃光电混合舱的物理信号研究

姓名：魏振宇

学号：519072910021

导师：徐东莲

学院：物理与天文学院（致远荣誉计划）

学科/专业名称：物理学

申请学位层次：学士

2023年06月

**A Dissertation Submitted to
Shanghai Jiao Tong University for Bachelor Degree**

Probing Physics Potential with TRIDENT hDOM

Author: Zhenyu Wei

Supervisor: Donglian Xu

Zhiyuan College
Shanghai Jiao Tong University
Shanghai, P.R.China

June 28th, 2021

上海交通大学
学位论文原创性声明

本人郑重声明：所呈交的学位论文，是本人在导师的指导下，独立进行研究工作所取得的成果。除文中已经注明引用的内容外，本论文不包含任何其他个人或集体已经发表或撰写过的作品成果。对本文的研究做出重要贡献的个人和集体，均已在文中以明确方式标明。本人完全知晓本声明的法律后果由本人承担。

学位论文作者签名：

日期： 年 月 日

上海交通大学
学位论文使用授权书

本人同意学校保留并向国家有关部门或机构送交论文的复印件和电子版，允许论文被查阅和借阅。

本学位论文属于：

- 公开论文
内部论文，保密1年/2年/3年，过保密期后适用本授权书。
秘密论文，保密____年（不超过10年），过保密期后适用本授权书。
机密论文，保密____年（不超过20年），过保密期后适用本授权书。

（请在以上方框内选择打“√”）

学位论文作者签名：

指导教师签名：

日期： 年 月 日

日期： 年 月 日

摘要

学位论文是本科生从事科研工作的成果的主要表现，集中表明了作者在研究工作中获得的新的发明、理论或见解，也是科研领域中的重要文献资料和社会的宝贵财富。

为了提高本科生学位论文的质量，做到学位论文在内容和格式上的规范化与统一化，特制作本模板。

关键词：学位论文，论文格式，规范化，模板

ABSTRACT

As a primary means of demonstrating research findings for undergraduate students, dissertation is a systematic and standardized record of the new inventions, theories or insights obtained by the author in the research work. It can not only function as an important reference when students pursue further studies, but also contribute to scientific research and social development.

This template is therefore made to improve the quality of undergraduates' dissertation and to further standardize it both in content and in format.

Key words: dissertation, dissertation format, standardization, template

CONTENTS

| | |
|---|-----------|
| 摘要..... | I |
| ABSTRACT..... | II |
| CHAPTER ONE INTRODUCTION..... | 1 |
| 1.1 NEUTRINO | 1 |
| 1.2 NEUTRINO ASTRONOMY | 2 |
| 1.2 NEUTRINO TELESCOPE OVERVIEW | 3 |
| 1. 2. 1 DOM..... | 3 |
| 1. 2. 2 Neutrino telescopes around the world..... | 5 |
| 1. 2. 3 Detection Principles..... | 9 |
| 1. 2. 4 Signal and Background for TRIDENT..... | 11 |
| 1. 2. 5 Trigger Overview..... | 13 |
| 1.3 PURPOSE OF STUDY | 18 |
| CHAPTER TWO TRIGGER STRATEGY..... | 20 |
| 2.1 TRIGGER STRATEGY DESIGN | 20 |
| 2.2 L1 TRIGGER | 21 |
| 2.3 L2 TRIGGER | 23 |
| CHAPTER THREE PERFORMANCE OF TRIGGER..... | 26 |
| 5.1 SIMULATION FRAMEWORK | 26 |
| 3. 1. 1 Analysis method | 29 |
| 5.2 BACKGROUND REDUCTION | 29 |
| 3. 2. 1Dark Noise | 29 |
| 3. 2. 2 K-40 | 31 |
| 5.3 SIGNAL EVENT EVALUATION | 34 |

| | |
|---|-----------|
| 3.3 SUMMARY | 37 |
| CHAPTER FOUR FUTURE IMPROVEMENTS AND OUTLOOK..... | 39 |
| 4.1 L1 TRIGGER OPTIMIZATION | 39 |
| 4.2 PHYSICS FILTER OPTIMIZATION | 41 |
| 4.2.2 Cylinder Method | 42 |
| 4.2.3 Particle Identification..... | 44 |
| REFERENCES..... | 49 |
| SYMBOLS AND MARKS APPENDIX 1 | 52 |
| RESEARCH PROJECTS AND PUBLICATIONS DURING UNDERGRADUATE PERIOD | 53 |
| ACKNOWLEDGEMENTS | 54 |

Chapter One Introduction

1.1 Neutrino

The neutrino is firstly proposed by Wolfgang Pauli in 1930 to fix the problem of energy and momentum non-conservation effect in beta decay.[1] In 1942, Ganchang Wang proposed the use of beta capture from ^{7}Be to experimentally detect neutrinos.[2] In 1956, the tiny particle is directly detected for the first time in Cowan-Reines neutrino experiment.[3] In the experiment, antineutrinos created in a nuclear reactor are captured by protons in 200 liters of water, and pairs of neutron and positron are produced, generating time correlated signals. The neutron is captured by 40 kg of dissolved CdCl_2 in water and the positron is annihilated by electron. This great breakthrough won the 1995 Nobel prize. This beautiful experiment is the prelude of all kinds of neutrino detections latter on.

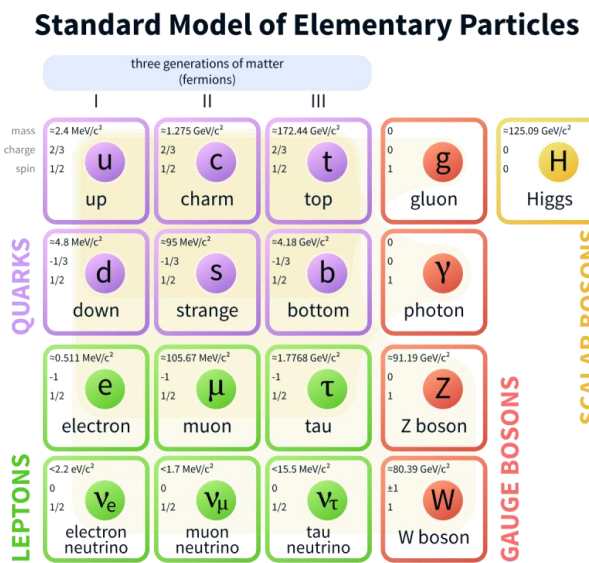


Figure 1 Standard Model. Neutrino is a kind of elementary lepton. (Source: wiki)

The neutrino is a kind of charge-neutral lepton with spin $1/2$, which is categorized in three different flavors: electron neutrino ν_e , muon neutrino ν_μ , tau neutrino ν_τ , shown in Figure 1. Since mass eigenstates and flavor eigenstates of neutrinos do not overlap, the probability of observing a certain flavor neutrino varies as it propagates (Flavor Oscillation Effect, 2015 Nobel Prize). [4]

Until this day, many scientific problems around neutrinos still wait for us to answer. Whether the neutrino is a kind of Majorana fermion is still elusive in science frontier up to now. If the neutrino is Majorana fermion, then the law of lepton conservation may be broken. New physics that is beyond

standard model is hidden behind. In experiments, observing neutrinoless double beta decay ($0\nu\beta\beta$) from N (A,Z+2) element decay is the key to uncover the mystery. [5]

1.2 Neutrino Astronomy

The neutrino only involves in weak interaction and gravity interaction. Its small cross section induces very scarce reaction events. So neutrinos are sometimes referred as ‘ghost’ particles since they penetrate most substances easily. This kind of nearly massless elementary particle is generated mainly in hadronic processes or nuclear reactions (beta \pm decay and electron capture), which is enriched in the nuclear power plant, celestial bodies, and earth atmosphere as high-energy cosmic rays Bombarding atmospheric atoms. The flavor, direction, and energy spectrum of neutrinos are widely different as the sources varies. Generally, high-energy neutrinos mark occurrence of violent hadronic processes. The processes can be summarized[6] as

$$\begin{aligned} p + p &\rightarrow \pi^\pm + X \\ p + \gamma &\rightarrow \Delta^+ \rightarrow \pi^+ + n \\ p + \gamma &\rightarrow \Delta^+ \rightarrow \pi^0 + p \\ \pi^+ &\rightarrow \mu^+ + \nu_\mu \\ \pi^- &\rightarrow \mu^- + \bar{\nu}_\mu \\ \pi^0 &\rightarrow \gamma + \gamma \end{aligned}$$

Compared to GeV and above high-energy photons which is deflected by pair-productions, neutrinos travel longer with less absorption or deflection in interstellar space. In universe observation, these oscillating high-energy particles can be utilized as a powerful tool to study the astronomical sources since neutrinos’ flavor constituents, direction, and energy of neutrino jets carry very rich physics information. Neutrino sources are widely considered as a smoking gun evidence for ultrahigh energy cosmic ray production, which is a centennial problem for human-being. In 2013, IceCube discovered a diffuse astrophysical neutrino with several potential sources included, such as active galactic nuclei, gamma-ray bursts, and starburst galaxies.[7] In 2017, IceCube linked observed high-energy neutrino with flaring blazar TXS 0506+056 with a 3.5 sigma confidence interval, which indicates an upcoming groundbreaking in multi-messenger astronomy.[8]

IceCube also carries out systematic searches for neutrino sources of different categories. Gamma Ray Burst (GRB)[9], Active Galactic Nuclei (AGN)[10] and Blazars[11], Galactic Neutrino Source[12], Fast Radio Burst (FRB)[13], Compact Binary Coalesces (CBC)[14] as well as Tidal Disruption Event (TDEs)[15] are all considered, while all final conclusions drawn from co-analysis up-to-now do not solve the puzzles completely. It seems that most of astrophysics neutrino jets may come from numerous weak sources, instead of dominant single source. High-energy neutrino source searching is still on the

way.

1.2 Neutrino Telescope Overview

These tiny particles are observed using extremely sensitive technologies in large volume. The secondary charged particles generated in neutrino-matter interactions induce detectable Cherenkov optical photons. A large body of target optical medium, such as sea water or Antarctic ice are continuously monitor by photon-sensors. This is namely the idea of building the massive Cherenkov optical neutrino telescopes to detect high-energy celestial neutrinos. In 1960, M. Markov published this breakthrough idea.[16] At the current level of human productivity, this is the only method to accumulate enough statistics.

1.2.1 DOM

Digital Optical Module, namely DOM, is the cell of the neutrino telescope. Deploying DOM arrays to detect Cherenkov optical photons is main body of neutrino telescope construction. Normally, (take DOM in IceCube as an example here) DOM is capsuled by a special glass sphere shell. The term ‘special’ here points to high pressure resistant (250bar for example, corresponds to 2.6km depth in seawater), high transparency in optical waveband, and low radioactivity to avoid extra background. A PMT or multiple PMTs are deployed in the shell.

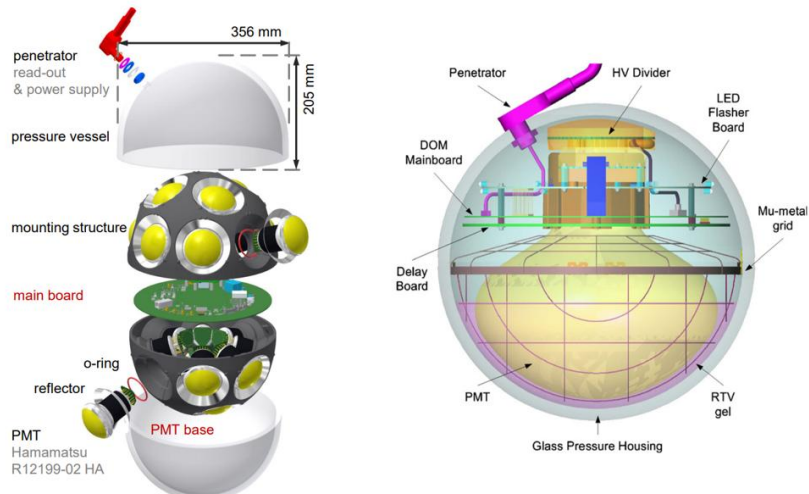


Figure 2 Left Panel: KM3NeT mDOM[17] (multi-digital optical module) internal design. Right Panel:
IceCube DOM internal design.[18]

In Figure 2, Optical gel (refractive index~1.4, very transparent) are added between PMT surface and the

shell to reduce photon loss. Large PMT also requires a metal net covering to shield geomagnetic field.

PMT, namely photomultiplier tube, multiplies the current produced by incident light (photoelectric effect in photocathode) by as much as tens of million times in multiple dynode stages, finally creates digitizable macroscopic electron current, which enabling single photon detection.

The main parameter of PMT is listed below:

1. Quantum Efficiency (QE): The probability that an incident photon in the photocathode can generate an electron. Normally, for 460nm, this number is around 30%.
2. Gain: Amplification factor that currents are gained after going through multiple dynodes.
3. Single photoelectron waveform: the waveform of a single photon. The key characteristic of the waveform are rising time, falling time and the peak amplitude.
4. Single photoelectron resolution: the peak-to-valley ratio between the single-photon peak and zero-photon peak in the charge distribution. This marks the ability of one PMT to distinguish single photon signals from baseline fluctuation.
5. Transient time spread: The full width at half maximum of transient time distribution. This quantity will in the end limit the angular resolution of the neutrino telescope.

Currents from the anode in the PMT will be digitized through electronics. Analogue Digital Convertor (ADC) or Time Digital Converter (TDC) will be implemented. This depends on certain circumstances. The former one can sample the waveform in a time interval. (For example, 500MHz ADC digitizes waveforms in 2ns time interval.) The latter one count the number of rising edge. Instead of the whole waveform, only the hit time and time-over-threshold or the amplitude will be transmitted.

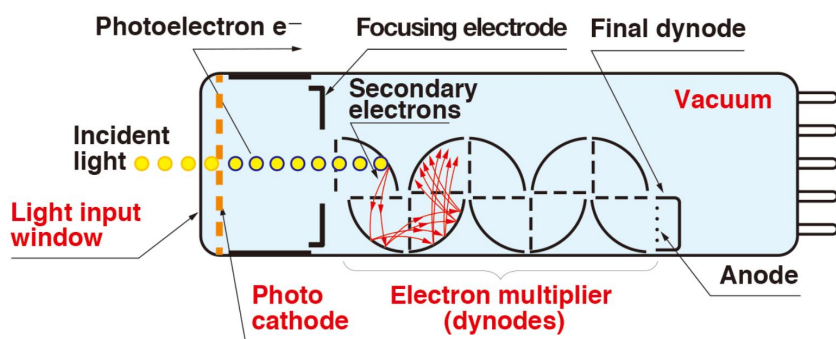


Figure 3 PMT working principle. [19]

High voltage ($\sim 1\text{kV}$) is applied in the vacuum tube. Currents from photocathode is multiplied level by level in several dynodes. Finally, they are collected in the anode.

New technique route of DOM has been developed recently. TRIDENT will incorporate SiPM with PMT to achieve high time resolution and detection efficiency. SiPM, silicon-photomultiplier, is a solid-state photodetector that can record single-photon signals through the internal avalanche process. The basic

unit of one SiPM is a single-photon avalanche diodes (SPADs) operating in Geiger mode. Each SPAD is connected to a quenching resistor. The scale of SPAD is a few micrometers (say 50 micrometers). For example, 3600 SPADs, connected in parallel, form a piece of 3mm by 3mm SiPM single piece. The avalanche process is pretty fast, on the level of hundreds of pico-seconds, since the space scale is around tens of micrometers, and the carrier's kinetic energy in silicon in the avalanche is around 1eV. (Normally, we exert the bias voltage ~50V.) This results in the excellent time sensitivity.

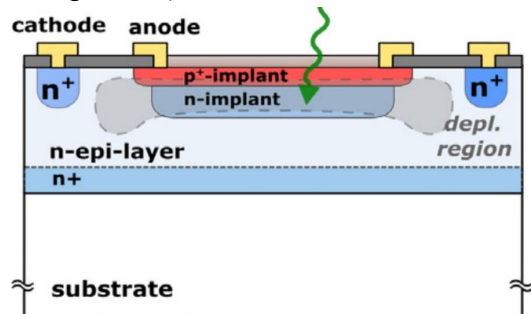


Figure 2 Working Principle of one SPAD. [20]

A bias voltage is applied in the P-N node and raise the carrier to a high potential energy. When photons outside come in, avalanche processes will happen.

As a Cherenkov radiation recorder, the following properties of the SiPM should be paid attention to.

1. Photon Detection Efficiency: considering both quantum efficiency and the geometry factor, this is generally the ratio of detected photons to the inject photons in one piece.
2. Dark Count Rate: the frequency of dark noise. This is in essence a thermal excitation process, determined by temperature. Since it is on the level of 30kHz/(3mm*3mm), the problem of pixel integration on large scale is still a frontier challenge. The dark noise will be superposed linearly.
3. Rising Time Jitter: The jitter of the rising time of the waveform. This value is similar to the TTS of PMT. The advantage of SiPM in the neutrino telescope is that the jitter is on the level of 10 pico-seconds, which brings to large improvement in the reconstruction.
4. Gain: The same as PMT. The ratio between the charge of output signal to the charge of the original photon-electron.
5. Cross Talk: When one pixel is triggered, it is possible that there is certain light emission process in the avalanche, and the adjacent pixel will be also triggered. One incoming photon will result in two or more photon electrons in the end.

1.2.2 Neutrino telescopes around the world

In 1998, theoretical calculations suggested that high-energy neutrino flux from AGN (Active Galactic Nuclei) jets or GRB(Gamma Ray Burst) can be observed by a cubic-kilometer detector with sufficiently sensitivity. Numerous interesting topics about cosmic neutrino, along with new physics beyond the

Standard Model and quantum gravity, can be studied through the neutrino telescopes. Several neutrino telescopes around the world are under development now. Their geometry design, technical route, noise source and the monitoring sky region are widely different. In this paper, neutrino telescopes point to digital optical module (DOM) arrays. Askaryan effect are also another method to observe neutrinos. These kind of neutrino telescopes such as GRAND[21] are not involved in here.

(1) IceCube

IceCube, located in the deep Antarctic ice, is the largest running Cherenkov neutrino telescope in the world. In the surface, IceTop possesses 81 stations and 324 optical sensors. Below the ice surface, 5160 Digital Optical Modules in total are deployed uniformly in 86 strings, monitoring one cubic kilometer volume. DeepCore, constituted by 8 strings with 480 DOMs, is designed for optimization of lower energies in IceCube experiment. Generally, DOMs form a uniform space lattice with translational symmetry mostly. The neighbor string distance is 125m and the vertical spacing of DOMs in string is 16.7m.

DOM in IceCube utilizes one 10-inch diameter PMT. The dark count, which is around 500Hz per DOM, is the main noise source on the DOM level. For a triggered (called hard local coincidence in IceCube) photon hit, the waveform will be read out in 300MHz sampling rate, while for un-triggered photon hit (isolated photons, called soft local coincidence in IceCube), only the time and amplitude will be read out. After event selections, 100GB/day data stream are transmitted to the north over satellite for further analysis.[22]

(2) KM3NeT

KM3NeT is a water-based neutrino telescope in the Mediterranean sea mainly driven by EU. Two clusters of strings form ARCA in Italy (Astroparticle Research with Cosmics in the Abyss). And one cluster constitutes ORCA (Oscillation Research with Cosmics in the Abyss) in French.

ARCA will possess instrumented volume of about 1 cubic kilometer with 230 strings comprised of 18 optical modules, slightly larger than that of the IceCube. ORCA will a total densely instrumented volume of about 0.0067 cubic kilometer. The construction of ARCA provides some valuable references for other water-based neutrino telescopes. They developed mDOM (multi-Digital Optical Module) with 31PMTs to detect neutrinos.[23]

(3) P-ONE

P-ONE (Pacific Ocean Neutrino Experiment) is located at a depth of 2660 meters in the Cascadia Basin. The geometry is designed in cluster shape. Each cluster has 10 strings equipped with 20 DOMs. The strings in one cluster form a double-ring structure, and the inner ring has radius 100m with 3 strings and the outer ring possesses 7 strings in the radius of 200m. The large detection array is composed of 7

clusters in total. The average distance between clusters is 1km. Their site is monitored by two pathfinder experiments named STRAW. The optical property of water and the environment parameters such as water velocity are evaluated. Their first prototype line is expected to be deployed in 2023.[24]

(4) Baikal-GVD

Baikal Gigaton Volume Detector (Baikal-GVD), with 192 modules successfully operated at a depth of 1.1km, is still under development. The start of Baikal-GVD can date back to 1980, when a laboratory of high-energy neutrino astrophysics was established in Moscow in USSR. They plan to finish the construction in multiple phases. NT-36, NT-72, NT-200 and NT-1000 is performed in sequence. They also implement the cluster-like shape design to adapt to the expenditure. The DOM used in Baikal-GVD only contains one large PMT, and the lake water does not contain any K-40, so its bandwidth is not that large. Since its depth is 1.1km, the rate of atmospheric muons is relatively large.[25]

(5) TRIDENT: the next generation neutrino telescope[26]

The tRopIcal DEep-sea Neutrino Telescope, TRIDENT for short, will be deployed on the abyssal plane at South China Sea. Since abyssal water, compared to the glacial ice of IceCube, contains less impurity, Trident will have added advantage in reducing photon scattering. Neutrino pointing in both the track and cascade channels can be benefitted. Also, since the latitude is low, TRIDENT can conduct the whole sky survey with the rotation of the earth.

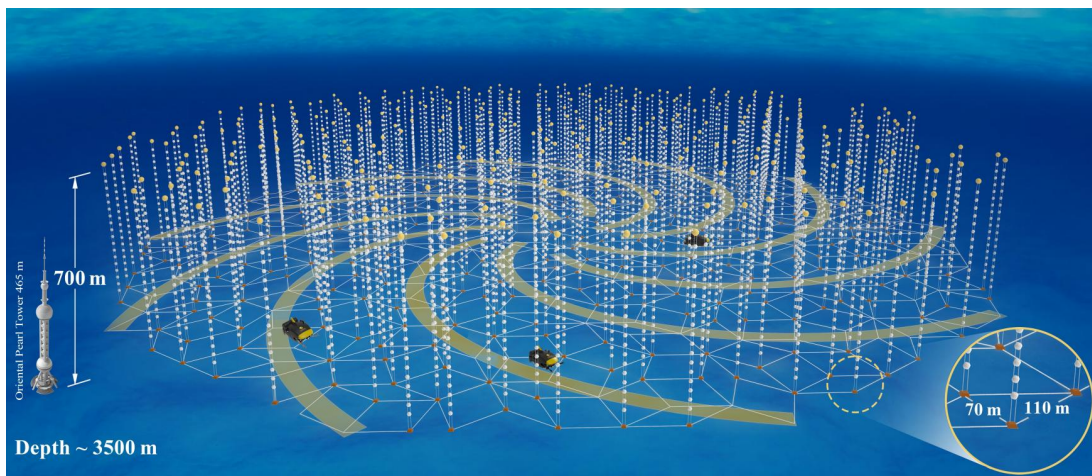


Figure 3 Rendering Diagram of Trident (Source: TRIDENT collaboration)

The telescope will have an Penrose geometry layout with 1211 strings and 22400 hybrid digital optical modules covering a volume of about 8 cubic-kilometer. Simulation shows that this kind of unsegmented geometry can reduce the clipping edge events, which happened in the edge of the detectors and more likely to occur in the clustering geometry. The spiral geometry can also deal with the ‘corridor events’, which referred to the events that pass through parallel arrays of strings in the detector. We also consider the requirement of ocean engineering when deploying the strings. ROV (Remote Operated Vehicle)

paths are left on the sea floor spirally. These ROV paths can help to conduct detector construction as well as long-term maintaining.

We also consider the layout of junction box system in the detector. Data transmission and power supply are implemented through junction box. Preliminarily, each sub-junction box point (triangle mark in the Figure 3) serves for adjacent 20 strings. The bandwidth and power consumption of strings will decide this number in future construction.

• String ▲ Junction box - - - ROV path

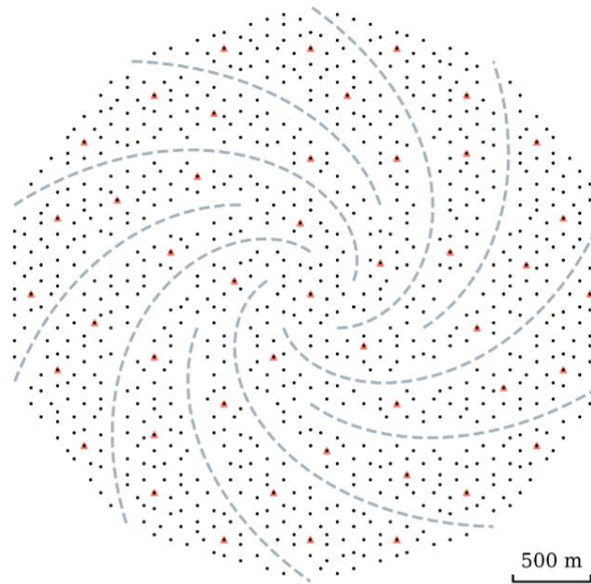


Figure 4 The layout of Trident. Penrose tilt is implemented. (Source: TRIDENT collaboration)

State-of-the art technologies will be included in hDOM (hybrid digital optical module) design. More than 30 3-inch PMTs and more than 20 1-inch PMTs or SiPMs will be integrated together to achieve high time resolution and excellent light collection ability. This next generation telescope carries more ability to pinpoint the astrophysical neutrino sources, as well as stays sensitive to all flavor neutrinos for multiple critical physics purposes.

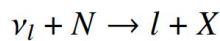
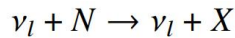


Figure 5 hDOM design picture. [27]

31 PMTs and 24 SiPMs are set in the layout in Figure 5. The simulation project introduced in the later chapter also comply with the design here.

1.2.3 Detection Principles

When high-energy neutrinos pass through the medium, deep-inelastic scattering (DIS) may occur between the neutrinos and the nucleus in the medium through the weak interaction. The secondary particles that are charged and largely boosted can be generated through DIS.



N is the nucleus, and l is the lepton. X is the hadronic cascade, full of pions and Kaons.

These high-energy secondary charged particles' velocity is very close to the speed of light, say c, in vacuum, which the light speed in water, normally $0.75c$, is significantly less than. Water is a common dielectric medium that can be polarized electrically. In the case, Cherenkov radiation effect can occur. Secondary charged particles carry the information from neutrino due to the conservation of energy and momentum, and emit a large amount of Cherenkov photons. The Cherenkov photons generated along the trajectory follow a fixed emission angle and can be captured by the DOMs in the neutrino telescope. This is the detection principle of neutrino telescopes. The well-known emission angle can be written as $\cos(\theta) = \frac{1}{n\beta}$. This angle property is the foundation of direction reconstruction in neutrino telescope.

The arrival time of a un-scattered Cherenkov photon in the detector can be written as

$$t_i = t_0 + \frac{z_i - z_0}{c} + \tan\theta \frac{r_i}{c} \#(I)$$

All quantities are marked in Figure 1. This expressions are applied in the likelihood method in the reconstruction and also the muon event filter algorithm (This will be discussed in later chapter). All photons emitted from the same muon track should obey the law of causality, when scattering effect does not slow down the average velocity too much. This property can be utilized to limit the direction range of muons before reconstruction.

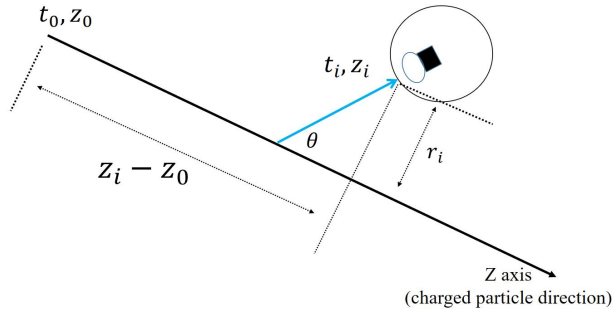


Figure 6 Cherenkov photon arrival time.

In Figure 6, the blue curve is the track of an emitted Cherenkov photon. θ is the Cherenkov angle. As for the energy spectrum of Cherenkov photons, the description is given by the Frank-Tamm formula.

$$\frac{d^2E}{dx d\omega} = \frac{q^2}{4\pi} \mu(\omega) \omega \left(1 - \frac{1}{\beta^2 n^2(\omega)}\right) \#(2)$$

This equation involves $\mu(\omega)$, the permeability, $n(\omega)$, the refractive index and q , the electric charge. It calculates the amount of energy emitted per travelling length and per frequency. Since the radiation energy is larger when β factor is closer to 1, more photons can be accepted by DOM for higher energy events. Also, more charged secondary particles can be generated from higher energy events. More photons received generally, more energy the particle carries. This lays the foundation for the energy detection in the neutrino telescope. According to the formula, the energy spectrum of Cherenkov photon is quite flat in optical region. Considering strong absorption effect of water in both large and small wavelength region, only wavelength around 450nm(blue light, 2.76eV) can mostly go through the medium. Since water only opens a window for the light from 2 to 3 eV, our PMTs and SiPMs inside the DOM should be sensitive to this wavelength band.

When substituting all constants in the Frank-Tamm formula and assuming the minimum ionization process, only considering optical photon part, we can obtain a simplified equation for rough estimation. Basically, losing each 2MeV when traveling along the trajectory, 200 Cherenkov photons can be generated.

$$\frac{dN}{dE_{deposition}} \cong 200 \text{ photons/MeV}\#(3)$$

Intuitively speaking, the signature of muon neutrino events, electron neutrino events, and tau neutrino events are distinguishable, since the properties of secondary particles are different. Muons, as well as some of tauons, travels longest, electrons bombard out a shower, and tauons both generate a shower and decay. Largely boosted muon neutrinos are viewed as the golden channel to search the astrophysical source in multi-messenger astronomy since muon tracks are usually very long ($O(1000m)$) and the reconstruction angular error is the smallest of all flavor. The angle between the induced muon and the neutrino can be approximated as the following expression:

$$\Delta\theta(\nu - \mu) \sim \frac{1.5^\circ}{\sqrt{E_\nu[\text{TeV}]}} \#(4)$$

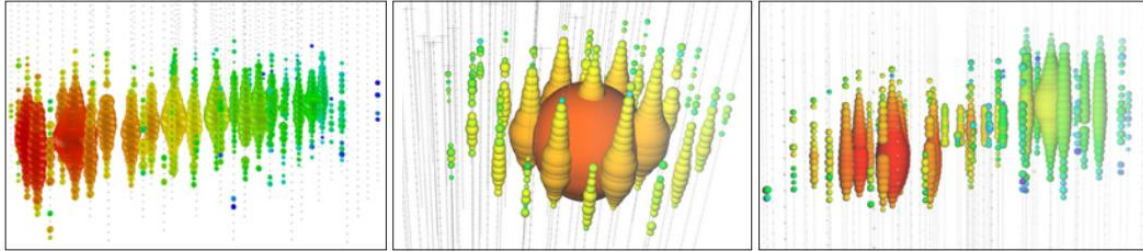


Figure 7 Three examples of event signatures in IceCube. [28]

In Figure 7, from left to right, a track-like event, a shower-like event, a simulated double-bang events are presented. They are considered as a muon event, electron event, and a tauon event. The DOMs are lightened by Cherenkov photons described above. The signature of events sometimes still degenerates.

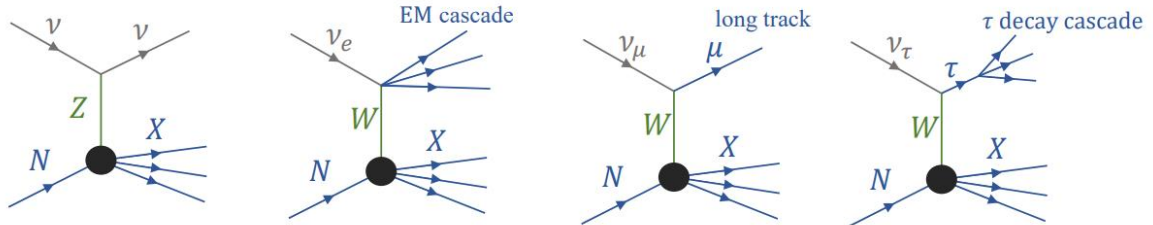


Figure 8 Feynmann Diagram of DIS. [29]

Figure 8 corresponds to the event signatures mentioned above.

The degeneration of signatures can still occur, since tauons can be track-like or shower-like. Clipping edge events only shed light on a few DOMs on the boundary, so it is not that easy to identify. Classification of particles is also a critical process in data analysis, where both machine learning and classical likelihood methods can be involved in.

1.2.4 Signal and Background for TRIDENT

In this paper, we generally refer the ambient noise such as K40 decay or bioluminescence and dark count as ‘noise’. K-40 and dark count are studied in detail. Atmospheric muons, neutrino events including all flavors, or other slow-moving heavy particles such as magnetic monopoles are called signals in general. Signals can be analyzed with multiple physics purposes, while noise should be reduced as much as possible to save bandwidth. This signal and noise definition is not universal, since ambient K-40 decay can also be studied as signal. We use this terminology in this paper for convenience, since neutrino telescopes core function is to study astrophysical neutrinos instead of K-40.

The bioluminescence at barren deep-sea plane is expected to be relatively small, because most

bio-activity is gathered in the sea surface. However, other neutrino telescopes has reported suspected bioluminescence signal which can still occupy large bandwidth in some cases. ANTARES in the deep Mediterranean Sea analyzed a 2.5-year long data and reveals that there might be several seasonal bioluminescence, lasting weeks long with up to two orders of magnitude higher than other background rate. It is a challenge for the workload of data transmission. As long as it is a uniform distribution in nanoseconds scale, we can still develop some trigger algorithms to reduce them. Their research also shows that the bioluminescence has strong correlation with temperature and current speed. Our TRIDENT lays in quite stable environment in terms of temperature and the current speed. This provides us an optimistic point of view to predict a low bioluminescence.

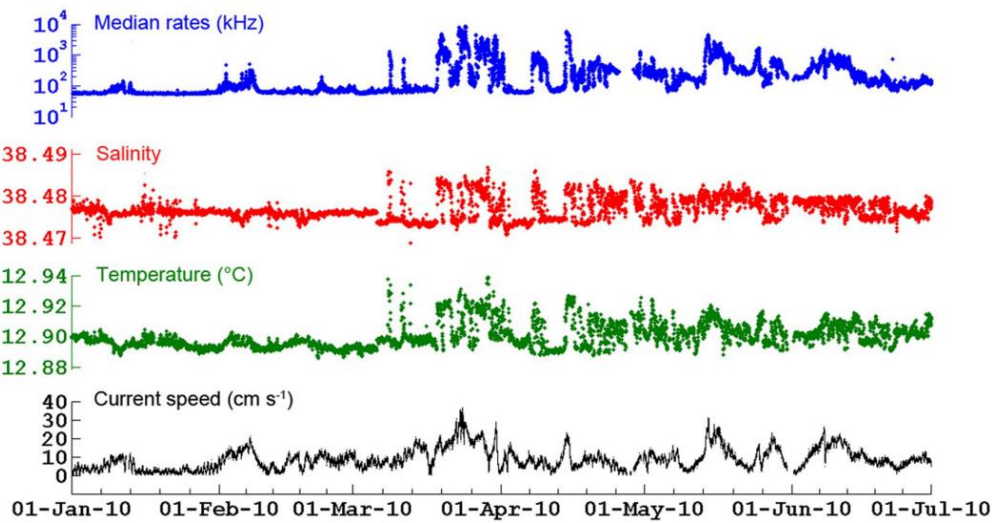


Figure 9 ANTARES claims that they have observed the bioluminescence. [30]

The data in Figure 9 is collected in around 2200m depth in seawater using several PMTs and other monitoring detectors. $\sim 100\text{kHz}$ baseline mainly comes from the K-40 decay. The median rates curve shows some correlation with other curves.

The element decay events in sea water are dominated by K-40. The activity is around 10.89Bq/L in the south China sea, according to [26].

The dark counts of photoelectric instruments are also a source of noise. Dark counts originate from the thermal excitations of the photocathode materials or silicon diode. For every 30-degree drop in environment temperature, the dark count rate drops by an order of magnitude approximately [31]. Low temperature ($\sim 2^\circ\text{C}$ in 3500 depth in the south China sea) can be a beneficial factor for noise reduction for the neutrino telescope. The rate of dark counts for one single PMT or SiPM is in a very wide range, in the order of 10^2 to 10^6 Hz, which is still quite sparse for nanoseconds granularity and tens of nanoseconds of trigger time window.

Currently, there are 31 3-inch PMTs and 24 3mm*3mm SiPMs or 1-inch PMTs in one hDOM. The dark

count rate of PMT and of 3mm*3mm SiPM is around 300Hz @ 2°C and 20-30kHz/9mm^2 @ 2 °C. Calculations show that after trigger, dark noise contributions can be down to $O(1)$ Hz , which is negligible.

Atmospheric muons from the bombard of cosmic rays on the atmosphere, neutrino events, and other rare events such as proton decays and magnetic monopoles are defined as signals. The atmospheric muons are dominate in this part. Thick water layers have already shielded most of the atmospheric descending muons, while still about 1000 muons per second arrive at the Trident detector. High energy up-going neutrinos are the most critical for future analysis, since it is most likely to be astrophysical since there are no other mechanisms to produce up-going high energy events. For relatively significance sources such as NGC 1068, Trident expects around one hundred observed neutrinos per year. In terms of bandwidth, descending muons occupy the overwhelming majority. Generally, neutrino events observed are categorized as three kinds. The visualization can be checked in Figure 7.

1. Track event: Charge-current muon neutrino reactions generate a high energy muon. A hundred-meters-long track will be left in the detector. Usually, these events are used to search sources since the reconstruction error can be controlled down to around one degree.
2. Cascade event: Charge-current electron neutrino reactions generate electrons. Or all flavor neutrinos in neutral-current channel react with nucleons.
3. Double-cascade event: Charge-current tau neutrino reactions generate tauons and a hadronic cascade. Then the tauons will propagate and decay, generating another cascade. The two cascades combined together are referred as the double-cascade event. The length of the tauon flight and the energy can be summarized as $l_\tau \cong 50m * \frac{E_\tau}{1PeV}$. So only when the energy is higher than hundreds of TeV can a distinguishable double-pulse signal be generated.

At TeV energy level, the flux of atmospheric muons can be 10^4 larger than astrophysical neutrinos. Up-going events are selected at first to reduce the atmospheric muons. Also, the starting-track event inside the detector can be chosen for astrophysical neutrino searching.

Generally considering the feature of noise and physics signals, the former one, generating single photon hits, distributes uniformly both in time and space, while the latter one produces multiple photon hits in a short time range in local hDOMs, which obey the law of causality.

1.2.5 Trigger Overview

It is a trend that the volume of the neutrino telescopes and the number of equipped photoelectric devices are becoming larger. The huge data amount will cause bandwidth overload and computation problems. Raw photon hits captured by DOM are almost 100% noise. The signal-to-noise ratio can be up to one in a million. Analysis of all datasets can be both unnecessary and impracticable without a trigger. So a

series of trigger strategies are implemented involving both software and hardware before analysis.

The basis of trigger is that signal and noise possess completely different time and space distributions. The noise is mostly uniformly distributed single photon events. While signals are generally multiple-photon clusters, much larger in terms of amplitude and the space-time correlation is quite unique compared with noise.

The general goal of trigger is the reduction of noise and the extraction of the physics. The second step is sometimes also referred as filter or event selection, since the bandwidth has already been suppressed by the first step, and particle identification are sometimes implemented in this phase. Trigger system decides whether a physics purpose can be captured by a neutrino telescope. Trigger is the start of analysis of all.

Design of trigger system demands the consideration of both the requirement of physics exploration and the engineering reality. Physics exploration asks for simulation and analysis, and the hardware engineering needs both skeleton design and test verification. Since the hardware design emphasizes the simplicity and the reliability more, less steps will be taken below the surface. All physics filters and particle identifications are more likely to be put on the computation station on the surface.

(1) IceCube

The DOMs used in IceCube contain only one PMT and no K-40 issue troubles the device. So inter-DOM triggers are not in need. IceCube defines two adjacent DOMs obtained photons in 1000 ns time window as Hard Local Coincidence (HLC) and isolated DOM hits as Soft Local Coincidence (SLC). All HLCs are digitized and full waveform will be read-out. For those SLCs, only the time stamp and the charge are read-out to save the bandwidth. For those high energy neutrino events, almost all waveform will be read out since most of photons will be HLCs.

All HLCs and SLCs will be transmitted above the ice surface into StringHubs. This computation station will process data with all kinds of filters to extract all kinds of track-like events and cascade-like events. The noise rate will be calculated and be used to monitor the status of the entire arrays. After the filter computing, 100GB/day's data is transmitted to the satellite. 25 filters in total are applied in this procedure. Each one is designed for a kind of physics signals searching. The total signal event rate for the entire detection array varies with time, since the atmospheric muon flux drifting from 2.5 kHz to 2.9 kHz seasonally, with a median rate value of 2.7kHz. The total DAQ (Data Acquisition) data rate, including both signals and noise, is approximately 1 TB/day.[22]

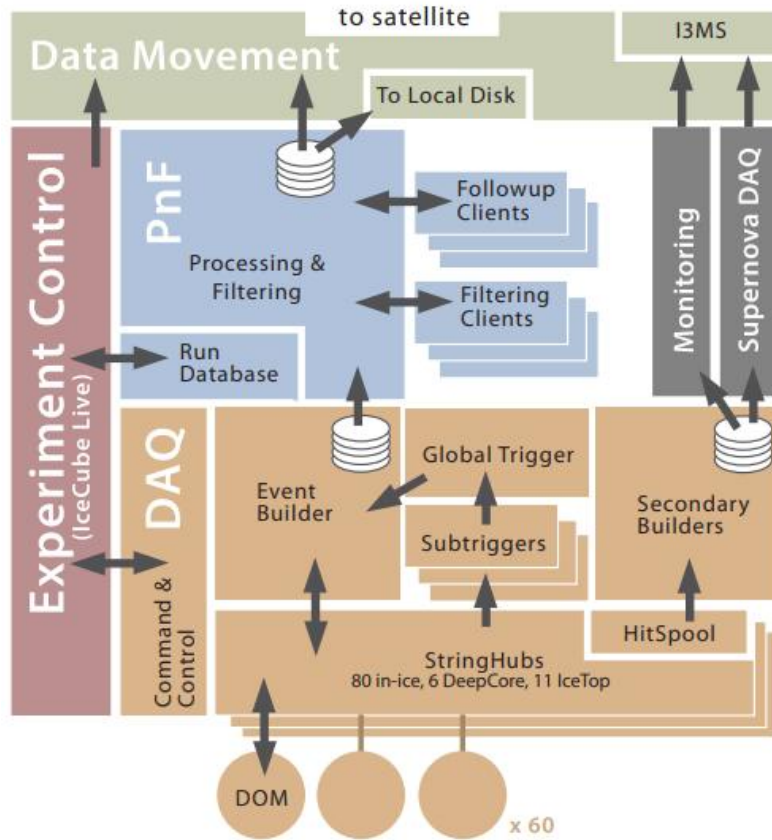


Figure 10 The data flow of IceCube. [22]

In Figure 10, StringHub can process non-physics data, which comes from monitoring and calibration, and sort raw physics data. Then HitSpool, a cache, queue all data, including those full waveform information, to serve for future requests from the Event Builder. Secondary Builders also possess functions for supernova events monitoring. It checks if the sum of data rate over a timescale is rising. If certain number condition is satisfied, further analysis will be implemented.

Filters set in IceCube serve for multiple purposes. SMT (simple multiplicity trigger) simply counts the number of HLCs in a certain time window. (say 8HLCs in $5\mu s$ for in-ice strings) Volume trigger requires 4 HLCs in $1\mu s$. String trigger requites 5 HLCs in $1.5\mu s$. Moreover, SLOP trigger (Slow Particle) are also designed for particles with velocity less than $0.01c$, such as hypothetical magnetic monopoles. The time window in SLOP is much larger than normal trigger frame, so the photon multiplicity requirement and the time-space requirement are both stricter. At least six photons which satisfy a certain ‘velocity condition’ are in need to activate a SLOP trigger. FRT (the fixed-rate trigger) reads out 10ms of hit data from the full detection arrays at a fixed interval for monitoring purposes. The detailed results is listed below. String trigger is used to count the photon in the same string, aiming to extract atmospheric muons. Volume trigger uses a fixed cylinder around photon hit clusters, which allows those low energy events which may not pass SMT trigger.

| Trigger | DOM set | N HLC hits | Window (μs) | Topology | Rate (Hz) |
|---------|----------|------------------------|---|--|-----------|
| SMT | in-ice | 8 | 5 | — | 2100 |
| SMT | DeepCore | 3 | 2.5 | — | 250 |
| SMT | IceTop | 6 | 5 | — | 25 |
| Volume | in-ice | 4 | 1 | cylinder ($r=175\text{m}$, $h=75\text{m}$) | 3700 |
| String | in-ice | 5 | 1.5 | 7 adjacent DOMs on a string | 2200 |
| SLOP | in-ice | $N_{\text{tuple}} = 5$ | $T_{\text{prox}} = 2.5, T_{\text{max}} = 500$ | $\alpha_{\min} = 140^\circ, v_{\text{rel}}^{\max} = 0.5$ | 12 |
| FRT | all | — | — | — | 0.003 |

Figure 11 The Trigger results summary from IceCube. [32]

In Figure 11, SMT is the single multiplicity trigger. SLOP is the slow particle trigger. FRT is the fixed-rate trigger. ‘N HLC hits’ denotes number of hard local coincidence.

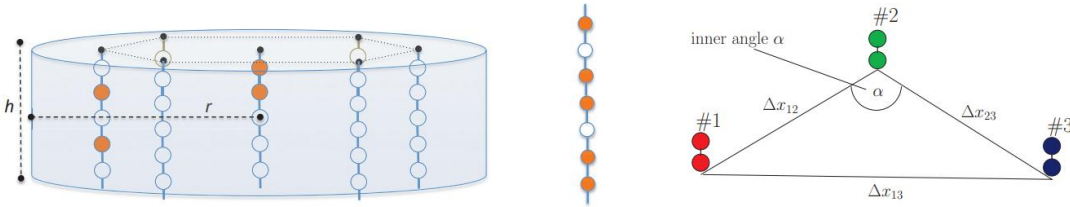


Figure 12 Volume, String, SLOP trigger illustration. [32]

The marks in Figure 12 corresponds to the ‘topology’ column in Figure 8. For SLOP, $v_{\text{rel}}^{\max} = 3 * (v_{12}^{-1} - v_{23}^{-1}) / (v_{12}^{-1} + v_{23}^{-1} + v_{13}^{-1})$, $v_{ij} = \Delta x_{ij} / \Delta t_{ij}$. This quantity should be small than 0.5 to pass the slow particle trigger.

(2) KM3NeT

KM3NeT first applies mDOMs in neutrino telescope. 31 3-incl PMTs are equipped together. Dark count rates are superposed linearly. K-40 decay events surrounded the mDOM can contribute 4-5kHz raw hit rate per PMT (ours is 2kHz per PMT[26]), and double photon hits ($\sim 1\text{kHz}$ per mDOM according to their simulation[33], corresponds to our tight L1 trigger, whose rate is $\sim 1.5\text{kHz}$ per hDOM) even triple photon hits also occurs steadily. This large noise hits force they adopt new read-out strategy. All waveforms are abandoned. Only the hits time and the time-over-threshold are recorded. The bandwidth is suppressed mostly in this phase. [34]

The upper limit of bandwidth of one mDOM is 1Gb/s. Usually, 9-12Mb/s output bandwidth per mDOM is occupied, dominated by K-40. Bioluminescence can occasionally boost the bandwidth by a factor of 10. [23]

The extraction of physics events is processed on shore in TriDAS[35] (the Trigger and Data Acquisition System, TriDAS). Different filters are applied parallelly. In the first step, they use ‘L1 trigger’ to process raw data. They preliminarily define L1 trigger as two components, simple coincidence and charge excess. Within a time window of 5ns, one or more hits on different PMTs in the same mDOM are

recorded, then it is a simple coincidence L1 trigger event. Photon hits with three photo-electrons charge is defined as a charge excess L1 trigger event. Latter on, they only use two photon hits in different PMTs in the same mDOM in 10 ns as L1 trigger. Charge excess concept is not in use in L1 trigger anymore.

The further process is named as ‘L2 trigger’. In this part, algorithms designed for several physics purposes work in parallel to select those more important photons hits clusters. L1 trigger already screens those isolated photon hits, which is mostly dark noise of PMT and K-40 hits. L2 trigger contains six parts.[35][36]

1. T-Triggers: two L1 events happen on adjacent or next-to-adjacent mDOMs in 200ns. Or two L1 events occur in the same mDOM in 55ns.
2. Simple causality filter: in a large enough photon hits set, check if photons in cluster satisfy

$$|\Delta t| \leq |\Delta \vec{x}| \cdot \frac{n}{c} \#(\mathcal{I})$$

This probably aims to search cascade-like events.

3. Sky scan trigger: divide the whole sky (4π solid angle) in around one hundred region. For each direction, check whether the photons in a large photon hits set satisfy the following inequation mutually:

$$|(t_i - t_j)c - (z_i - z_j)| \leq \tan\theta_c \sqrt{(x_i - x_j)^2 + (y_i - y_j)^2} \#(\mathcal{Z})$$

θ_c is the Cherenkov angle. (x_i, y_i, z_i, t_i) is the space-time coordinate of photon i. Z axis is the direction pointing back to the sky region. The coordinate system is rotating when checking different directions. The calculation is done by assuming the coordinate system is aligning with the muon track direction. This trigger aims to select a direction if photons come from muon track events. Only when the checked direction is close to ‘the real direction’, the above equation can be satisfied. This trigger serves for the reconstruction of muon tracks in the next phase.

4. Tracking trigger: the specific calculation is the same with the sky scan trigger. The direction here is not from divisions of sky region. Instead, it comes from certain sources such as NGC 1068.
5. Vertex splitting trigger: Use inertia tensor of photon hits coordinates to check if photon hits are cascade-like or track-like. Calculate inertia tensor is simple and fast, which can save some time for detailed reconstruction. For example, if photon hits are very track-like, then cascade reconstruction will not be implemented for economizing computing space.
6. External trigger: alert message from other telescopes. For example, Gamma Ray Bursts were captured by some satellites.

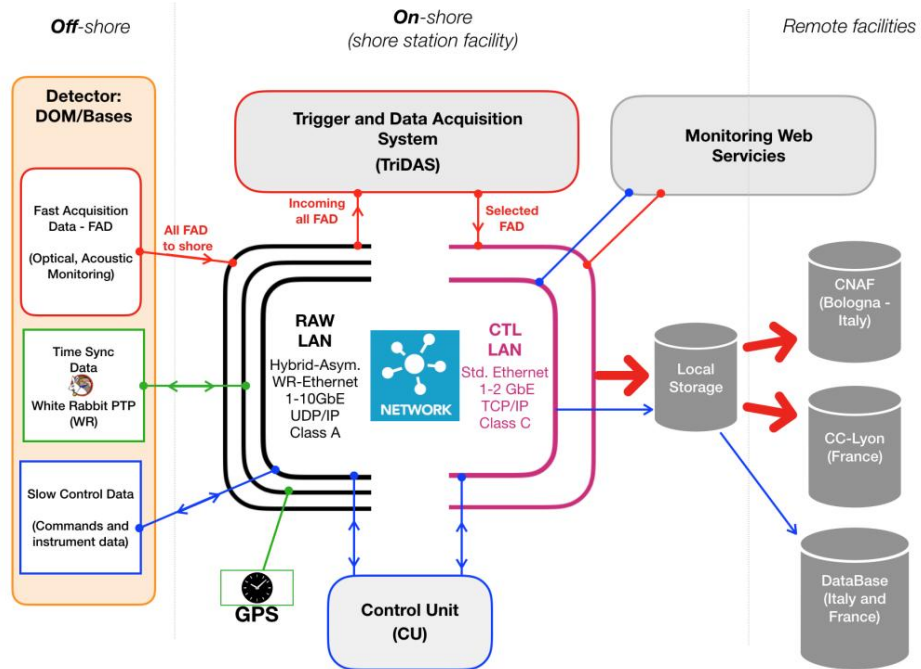


Figure 13 Framework of data system for KM3NeT. [33]

In Figure 13, from left to right, data flow from the front end to the final analysis are presented. Photon hit, acoustic data, positioning data and time synchronization system as well as instrument data are transmitted to shore station via RAW-LAN. TriDAS on shore will implement software trigger, including L1 and L2 trigger.

(3) Baikal-GVD

In lake water, salt such as K-40 is barely contained, so the noise bandwidth is not super high. Relatively simple and fast methods are adopted when designing the data acquisition system. The trigger in the data acquisition system operates in two modes, L trigger and L&H trigger. The previous one demands coincidences of signals in the selected time interval, and the latter one asks for coincidence in any adjacent optical modules. [37]

1.3 Purpose of Study

Even though noise contributes most in total bandwidth, and atmospheric muons contributes most in signal bandwidth, we should transmit all data to avoid the loss in physics information and be careful when reducing the background. Those relatively low-energy events (sub-TeV) may create only a few Cherenkov photon hits, which is not significant enough to be distinguished from K-40. Even If the

photons' distribution in time and space are quite dense when the energy of neutrino events is high, those hDOMs far from the event vertex still capture few photon hits, which may cause misjudgment in extracting signals. The more stringent criterion we choose to suppress noise, the less pressure we face to transmit data, and the more physics loss we will face.

The purpose of this work is to explore the possible way to reduce the background as well as to make sure signals are not impaired. hDOMs in TRIDENT are equipped with most number of PMTs and SiPMs, than any other DOMs ever designed. Former neutrino telescopes are generally designed with the 'all-data-reserved' philosophy. As much as possible information is reserved when outputting the data to shore from DOMs. This strategy can be helpful to the simplicity and reliability of hardware design inside the DOM. And all information are reserved to the data station on shore, which avoids the potential loss of physics information. While, on the other side, this strategy is a waste of bandwidth. Retaining all noise in the cable is not necessary.

The next-generation neutrino telescope, Trident, may not be able to apply the same methods to transmit and digitize data, since the bandwidth is unprecedently high and the monitoring volume is incomparably large. New ways of trigger are in need to adapt to the current level of data transmission and computation. In one hDOMs, 55 photon sensors (31PMT+24SiPM) are applied. Without any raw data process, all digitized photon signals will occupy 2GB/s for one hDOM, which is 35TB/s for the large detection arrays. It is not a treatable data amount in this era. My work focuses on the hDOM internal trigger. The raw data will be suppressed and selected inside hDOM using our designed trigger algorithm. Interested physics signals, which only takes up very little bandwidth, should be retained as much as possible, while the noise should be abandoned. The detailed evaluation of our trigger algorithm in background suppression and physics loss will be presented in this paper.

Chapter Two Trigger Strategy

2.1 Trigger Strategy Design

The trigger strategy design of Trident should not bear any physics loss, at the same time, suppress the bandwidth to satisfy the workload of data transmission. In one hDOM, 31 PMTs and 24 SiPMs are equipped. Large bandwidth from numerous photon sensors demand relative strict trigger criterion.

The framework of trigger constitutes two level. The first level is hDOM-internal trigger, abbreviated as L1 Trigger. It is the first stage to suppress the bandwidth by considering the number of PMT photon hits. The second one is referred as physics filter, generally called L2 Trigger. This part considers photon hits in adjacent or next-to-adjacent hDOMs. Physics signals will be extracted in this stage since photon hits are related mutually in space and time.

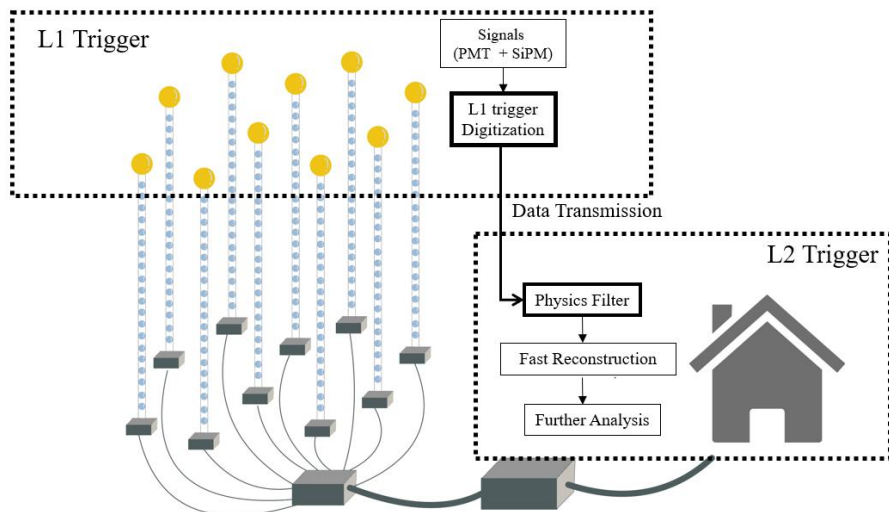


Figure 14 Conceptual Framework of our data system.

For the trigger system discussed in this paper, hDOM Internal Trigger (L1 Trigger) and Physics Filter (L2 Trigger) are two main components. Updated position information will be appended in the dataset on shore for calculations in physics filter. The White Rabbit clock synchronization system are not involved above. In Figure 14, from left to right, hDOM side, transmission site and on-shore site are listed in order.

Data from a local cluster of hDOMs, such as a hDOMs inside a cylinder or a sphere space will be extract for next-stage reconstruction. Some of the particle identifications can also be implemented in

this phase. This part of trigger is finished at the on-shore station. Principally, in the junction boxes, part of these works can be conducted. While considering the engineering below the sea surface should be as simple and reliable as possible, we probably move the complexity on shore.

2.2 L1 Trigger

L1 trigger decisions will be made by only PMT. Since the dark count rate of SiPM is in the order of $O(10^6)$, the trigger of SiPM is not very practical. Trigger in this level is implemented inside hDOMs. The waveform of L1-triggered events will be read out for particle identification and reconstruction.

The implementation of the L1 trigger is summarized as follows:

1. If at least two different PMTs receive at least two photons in 10ns, then it is an L1-triggered event.
2. The waveform of a total of 1000ns will be read out. The first 300ns is before the L1-triggered event and the second 700ns is after L1.
3. The 1000ns read-out time window is for the entire hDOM, including 31 PMTs and 24 SiPMs.

We expect that this part, the foundation of all later data processing, will suppress background, and make no influence on the physics events. A detail that needs to be emphasized is that only two different PMTs are hit, it is an L1 trigger event. This is a tight version of the L1 trigger. It is also acceptable to loosen the criterion by allowing the two photons distributed in the same PMT. We will evaluate both the tight version of L1 (two photons in different PMT) and the loose version (two photons can be in the same PMT).

Other neutrino telescopes transmit all data to the shore and then use a series of triggers to process data. However, since the bandwidth of Trident is super high($O(TB/s)$, for all waveforms without trigger) and the workload of optical fiber in the sea cable is limited, we may design an FPGA inside each hDOM to process this L1 trigger. All the signals will be stored in analog form in a buffer. When the coincidence condition computed by FPGA is satisfied, the triggered signals will be digitized by ADC and transmitted by cable. Otherwise, only the time and the charge of a hit will be obtained by TDC and much less information is transmitted. The physics loss in this phase is unretrievable, the criterion design must be very careful.

It is an obvious drawback that only two or more than two photons can form an L1 trigger. Single-photon condition can never satisfy the L1 trigger. This single photon from physics events can still carry some information that may be helpful for energy and direction reconstruction. Since the dark count and most K-40 decay generate single photon hit, it is quite difficult to distinguish a photon's origin. A possible

solution is that when a higher-level trigger is satisfied, all data from the entire detection array or a large cluster of hDOMs are read out. Moreover, TDC readout method should also be considered, because the bandwidth from TDC is quite small. L1 trigger itself cannot save single photon from physics signals. A no-loss solution of readout method can be proposed:

4. No-trigger readout of the TDC information of PMT (preliminary estimation result of this part of bandwidth is 20MB/s/hDOM)
5. When the number of PMT coincidence photon number is greater than 2/3/4, PMT waveform ADC readout + SiPM TDC readout (bandwidth estimation will be discussed in the latter chapter)

The specific number will be determined by the bandwidth upper limit.

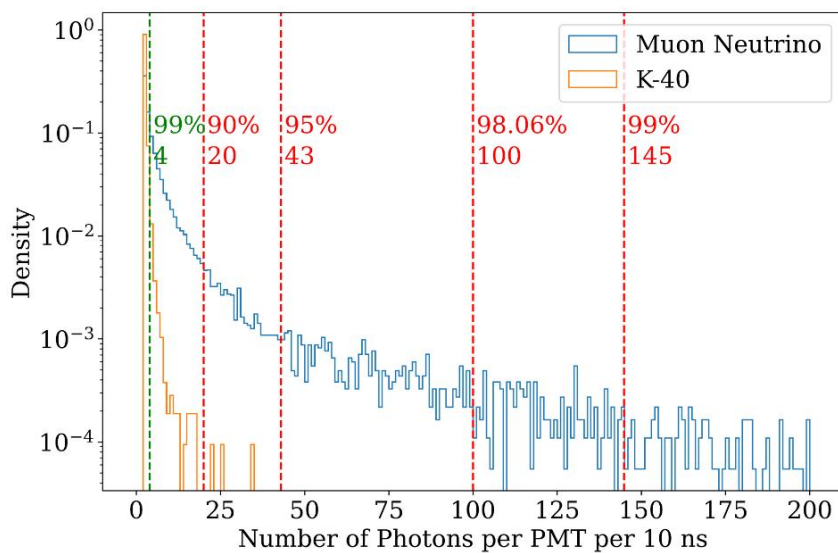


Figure 15 The photon number distribution for a single PMT in 10 ns trigger time window.

In Figure 15, 10k muon neutrinos ranges from 1TeV to 10 PeV are simulated. The number of landed photon is much larger than the K-40 events. This characteristics of photon multiplicity is the foundation of our L1 trigger. K-40 events mostly generate less than 4 photon hit, while muon neutrino events can generate up to hundreds of photon hits.

The implementation of L1 Trigger relies on electronics design. The general framework of electronics is described below.

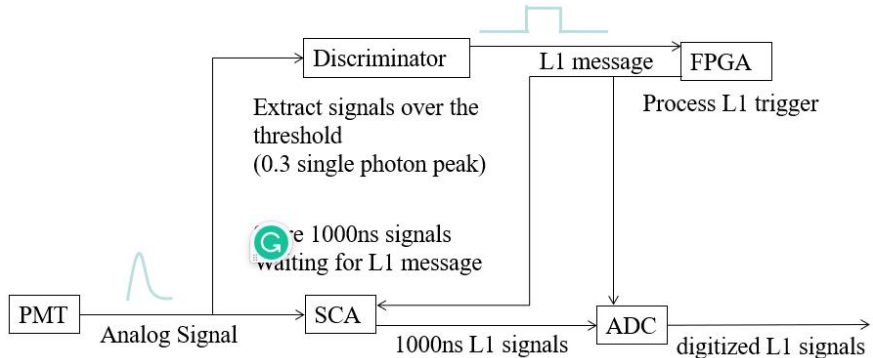


Figure 16 The conceptual framework of electronics.

In Figure 16, PMT works as the signal source and SCA works as a buffer. The discriminator processes the signals whose peak value is high enough and FPGA implements the L1 trigger. In FPGA, time information will be included. If two rising edges are found in the time window, then the L1 message will be transmitted to the SCA and ADC. 1000ns waveform will be digitized.

It is worth mentioning that when ADC reads triggered data from SCA, time consuming is around three times of trigger time window, which is 1000 ns. So 3000ns dead time is expected for each L1 trigger, due to the read-out process of ADC.

2.3 L2 Trigger

L2 Trigger is generally referred as physics filter. The main purpose of this part is to extract physics signals. This part is the subsequent procedure of L1 trigger and the guiding process before reconstruction. The function will be implemented in the computation infrastructure on the shore. The idea can be generally summarized as convex envelop search. For a series of photon hits distributed in 3D space and time(4 dimensional linear space), we should find a boundary to capsule all points without physics loss by considering the characteristic of physics signals, and the boundary should be as small as possible to reduce data amount.

For muon neutrino events, tau neutrino events, electron events, and atmospheric events, the signatures are widely different. Different reaction channels and different energies of the event corresponds to different size of boundary. Normally, for a 100TeV shower event, tens of hDOMs will be lightened. For 100 TeV track event, hundreds of photons will land in tens to hundreds of hDOMs. Time distribution for single PMT ranges from ten to one thousand nanoseconds. This feature requires that the physics filter should be loose and run in parallel to involve all situations. A strict ‘envelop’ involving all hits without redundancy is not practical without detailed reconstruction. Physics Filter phase does not involve complex computation. Simple and fast methods should be developed.

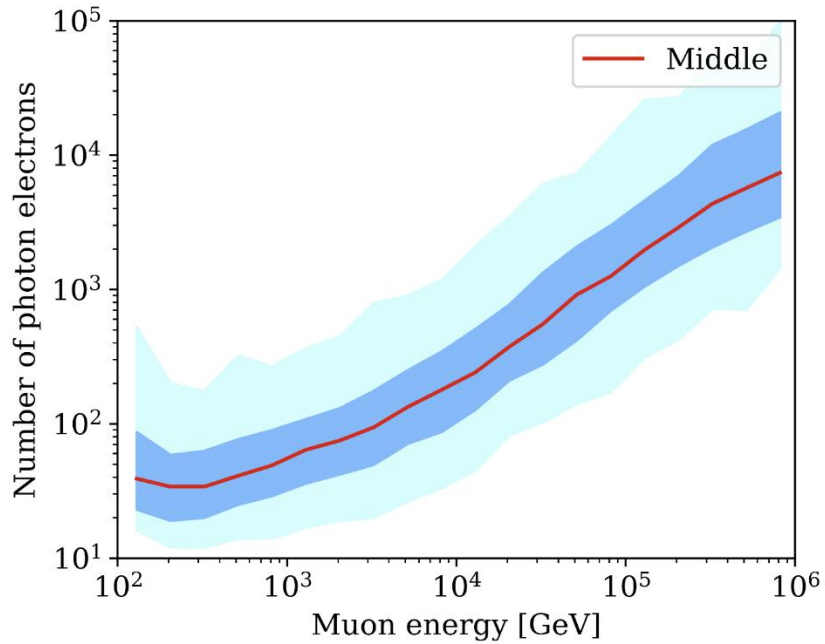


Figure 17 Number of photons received from muon events from simulation. (source: Trident collaboration)

In Figure 17, the nearly linear blue band are expected since the number of photons should be approximately proportional to the energy. But we can conclude that the photon number is distributed in very wide range for the events with the same energy. The wide distribution leads to relatively loose parallel physics filter. Some sparse photon events can still be very high energy.

We can first use an inter-hDOM trigger to mark those corelated events, which is an indication of physics signals. The inter-hDOM trigger's idea is basically the same as L1 trigger. It only considers the coincidence between 2 adjacent or next-to-adjacent hDOMs. If two L1-triggered hDOMs are adjacent or next-to-adjacent within around 1000ns, then these two hDOMs are inter-hDOM triggered. Inter-hDOM triggered events are a strong indication of physics event instead of ambient noise.

Cylinder method and sphere method are proposed as preliminary solution for muon events and shower events. Once there are multiple I events or mixing of L1 and I events in the same cluster, these methods can be applied to the cluster of data for latter analysis.

(1) cylinder method

The idea of the cylinder method is that photons from track-like events propagates within several times of absorption length of seawater. It is very safe to argue that almost 100 percent of direct photons are constraint in the length of 5 times of attenuation length (99.32% around 100m). So for track events, hDOMs in a large cylinder can involve all physics information. In this sense, data from only a proportion of detection arrays is processed. This helps to release the pressure of latter reconstruction

computation. The direction of the cylinder can be selected from simply calculate the expected arrival time of photons. The complexity of the calculations is $O(n)$. The calculated value should be close to the real occasions. The vertex of the muon track can simply use the center of mass of photon hits.

(2) sphere method

For cascade-like events, electrons and gamma rays generate large optical photon shower within tens of meters. The photons from same events all obey the law of causality since they originate the same high-energy particle. When the number of L2 events occurs and their maximum distance is smaller than a certain value, data from hDOMs inside a sphere will be transmitted for reconstruction. The radius of sphere will be a redundancy length (for example, 100m) plus the maximum distance from the center of mass to the photon hits point.

In essence, these two methods rely on the characteristics that all physics events are local. A portion of hDOMs is enough to include all information. So not all hDOMs are used for reconstruction. The preliminary quantitative discussion is in the latter chapter.

Chapter Three Performance of Trigger

The quantitative evaluation of the hDOM internal trigger (L1 trigger) is presented in this chapter. We conduct a Geant4 (a platform in C++ using Monte Carlo methods to describe the passage of particles through matter) simulation to test its background suppression ability and the physics loss due to the trigger. The bandwidth estimation of both noise and signals is also conducted for the guidance of hardware design. The upper limit of bandwidth should be in the range of the workload of our data system. The data amount in the future detection array should be computable and transmissible. Also, theoretical calculations are conducted specifically for dark noise.

5.1 Simulation Framework

In our simulation framework, we construct one hDOM in the center of a sphere water world. When muon events are injected, the radius of the water world is 100m. When K-40 events are sampled, the radius of the water world is only 30m, since most coincidence events are in very short-range limits. Cherenkov radiation can be generated in the process and captured by the PMTs inside the hDOM in the center. When the Cherenkov photon hits the PMT surface, their time, energy, and PMT ID will be stored in a root file. A Python analysis program will apply the L1 trigger algorithm to the dataset generated from Geant4. The purpose of the framework is to generate simulation signals and noise in one hDOM, and apply the trigger algorithm with adjustable parameters such as the time window, to finally evaluate the general performance of a certain set of parameters. The parameters of the L1 trigger are named as the coincidence photon number α and the time window β . If α photons are captured in β ns, then the hDOM is L1-triggered. The difference between the two versions, namely the requirement of different PMTs, of the L1 trigger will also be discussed. And a 1000ns length digitized signal will be transmitted.

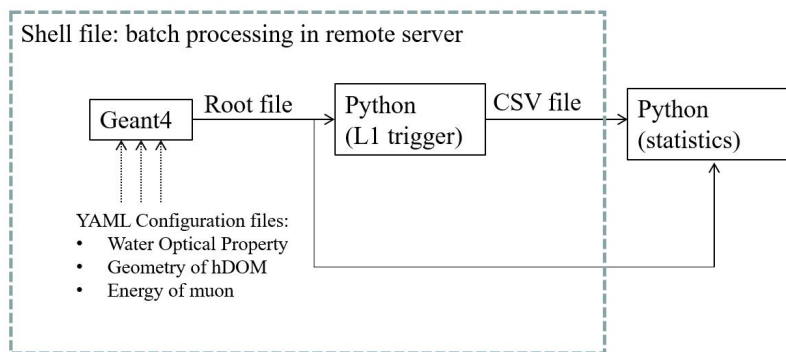


Figure 18 Workflow of the simulation project.

The geometry layout of PMTs and SiPMs in hDOM, muon energy, and the water optical property are

adjustable. Batch processing, which helps to significantly reduce the running time, replaces parallel computing to some extent.

The optical property of seawater including phase refractive index, Rayleigh scattering length, Mie scattering length, Mie scattering angle, and absorption length is set for all wavelengths. The group refractive index can be automatically processed by the Geant4 build-in function.

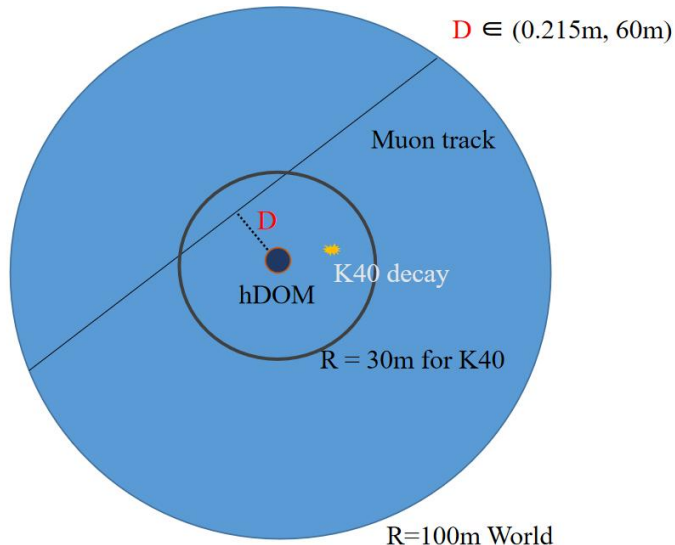


Figure 17 Geometry of Geant4 simulation project.

The geometry of hDOM is set basically the same as the situation in Figure 3. The outer glass shell, optical gel, and part-sphere-shaped PMTs are established.

For K-40 decay events, there are two branches. 10.698% of events generate 1.459 MeV mono-energy gamma rays (electron capture, $K40 + e^- \rightarrow Ar40 + \gamma + \bar{\nu}_e$), and 89.302% of events generate electrons (beta decay, $K40 \rightarrow Ca40 + e^- + \bar{\nu}_e$). The energy of electrons ranges from 0.1MeV to 1MeV. Other secondary particles such as neutrinos are not observable. Gamma rays will transfer energy to electrons by Compton scattering, which finally leads to Cherenkov radiation. The source of optical photons in essence is around ten percent gamma rays and ninety percent electrons. So we inject electrons and gammas corresponding to the branching ratio and energy spectrum to simulate the decay events. As for the position of the decay events, uniform distribution in 3D space is assumed. The seawater is homogeneous in terms of radioactivity.

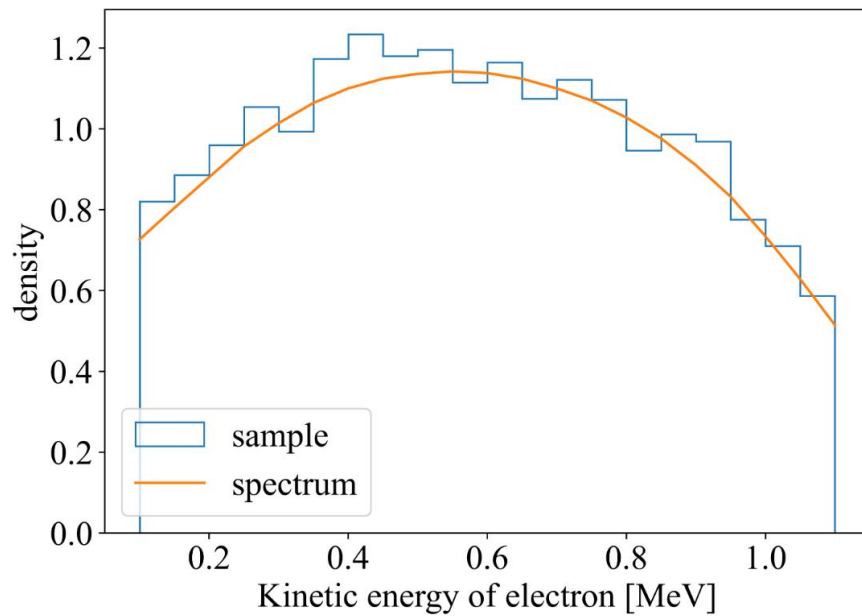


Figure 19 kinetic energy spectrum of electrons from K-40.

The yellow line is from theoretical results. The histogram is sampling results from the Geant4 simulation. Most of the electrons possess enough energy to emit Cherenkov radiation. The Cherenkov radiation threshold for electron is 0.265MeV in water.

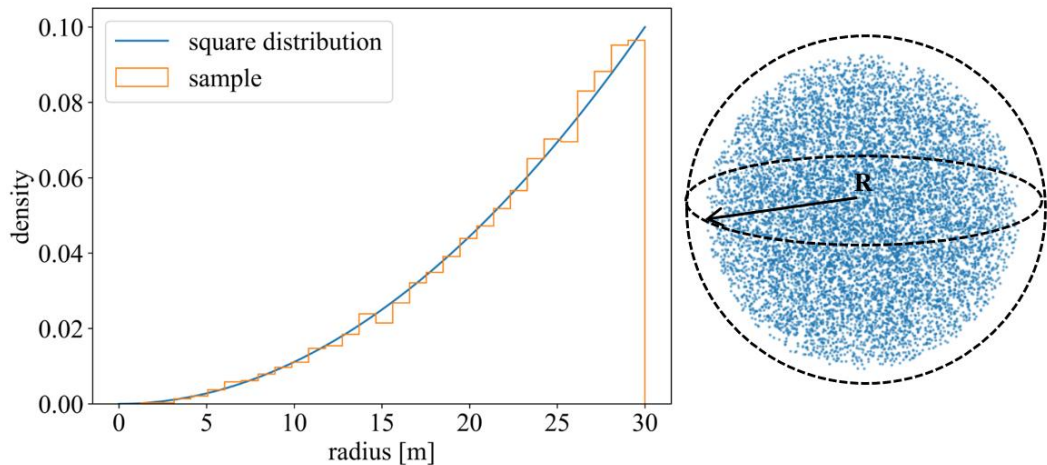


Figure 20 The position sampling of K-40 decay.

In Figure 20, the left panel is theoretical results of square distribution and the sampling result. The radius of uniform positioning in a sphere should obey square distribution. The right panel is 3D scatter visualization of the sampling result.

For the muon track, the distance from the hDOM to the track and the energy can be manually adjusted in each simulation. The direction of muons is uniformly distributed. We focus on the distance at around

30m and the energy is around hundreds of GeV to several TeV. Since this part is the subtlest region. When the energy is higher, or the distance is closer, the specific trigger algorithm does not matter anymore, since the event is bright enough.

3.1.1 Analysis method

To process the root file from Geant4, a Python script is created. Part of the photons are abandoned according to the quantum efficiency property of PMT. Then the photons are sorted by the arrival time in ascending order.

Then, in order to check if there are α photons in β ns, the time difference of the previous photon and the latter photon is calculated. The complexity of this step is $O(n)$. Secondly, we check if the sum of $\alpha - 1$ intervals is smaller than β ns. If it is smaller, then an L1 trigger event is set. All photons within 1000ns time window will be labeled as L1 photons. It is very fast if the numpy or pandas package in Python is included in the second step since they all run in parallel. If the coincidence photons are required to fall on different PMTs, an additional ‘if’ statement is implemented.

The PMT ID of L1 photons is sometimes also put in use. Since we may pick up the photons landed in adjacent PMTs for other analysis purposes.

All L1 photons will be selected and stored in another CSV file for latter analysis. The rate of the K-40 L1-trigger event is calculated by the number of L1 photons divided by α . As for the success ratio of muon events, we check if a muon can generate L1-triggered photons. If there is, then the muon is labeled as successfully L1 triggered. The success ratio of muon events is calculated by the L1-triggered muon divided by the total injected muon.

The Python script can process different α and β in parallel. The most time-consuming process in the analysis generally is readout and write-in procedure. The total run time in the server is controlled down to several seconds for one single (α, β) set. We scanned the phase space of L1 trigger (α, β) set.

5.2 Background Reduction

3.2.1 Dark Noise

This part is conducted by theoretical calculation. Dark noise, or dark count, is the inherent thermal property of photon sensors. We assume the frequency of the dark noise is f . This number is 300Hz/PMT or 300kHz/9mm² SiPM at around 2 degree in Celsius(deep sea temperature from experiment). And the

time of dark noise photon is sampled in uniform distribution. The probability to expect α photons in β ns is described by the integral of the gamma distribution. L1 false trigger rate R by dark noise is given below.

$$R = f \int_0^{\beta} \Gamma\left(\alpha - 1, \frac{1e9}{f}\right)(t) dt \#(1)$$

The $\frac{1e9}{f}$ parameter is the expected time interval between two dark photon hits. The parametrized Γ function is defined as:

$$\Gamma(a, b)(x) = \frac{b^a x^{a-1} e^{-bx}}{\int_0^{\infty} t^{a-1} e^{-bt} dt} \#(2)$$

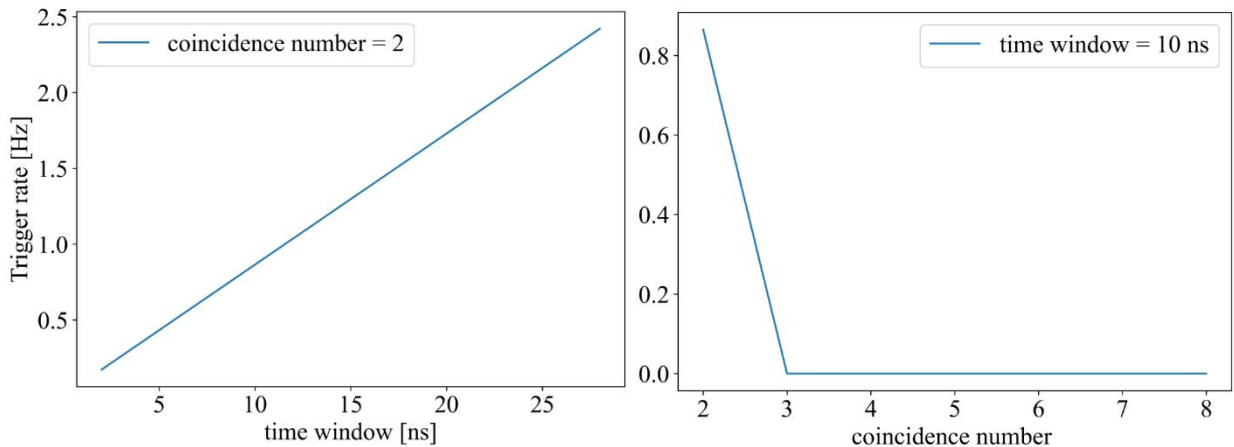


Figure 21 Dark noise L1 Trigger rate

In Figure 21, the right panel is the trigger rate versus coincidence number α . And the left panel is the trigger rate versus time window β . At most, when $(\alpha, \beta) = (2, 30)$, the trigger rate is 2.4Hz, three orders of magnitude smaller compared with K-40. For those coincidence photon number is larger than 2, the trigger rate is negligible. When $(\alpha, \beta) = (3, 30)$, the trigger rate is 0.00005Hz.

The calculation above does not consider the requirement that two photons should be in different PMTs. It is the loose version of L1. Even though we choose the loose version, the rate is still negligible.

The difference between the loose and tight versions of L1 on dark noise is quite small in fact. It is quite rare that two coincidence photons happen in the same PMT among 31 PMTs, so whether or not to regulate the two coincidence photons occur in different is not important at all. Probability calculation

shows that there is only a $\frac{1}{30}$ relative difference between the two versions of L1.

3.2.2 K-40

The K-40 decay events are the most dominant noise source for TRIDENT. So we should understand the behavior of hDOM response to K-40 well. The activity of K-40 is around 10Bq/L (10.87Bq/L as simulation input in this chapter), and seawater within tens of meters can contribute to photon hits. The Cherenkov threshold for electrons in seawater is around 0.3MeV. Most electrons from K-40 decay can generate numerous optical photons by Cherenkov radiation. This leads to the result that the rate of noise hit from K-40 can reach up to around 60k Hz per 31PMTs in one hDOM (2.02 ± 0.09 kHz per PMT), according to the previous simulation result. We generally present the results analyzed under the loose version of L1. The different PMT condition is not added. This shows the lower limit of the background reduction ability.

After L1 Trigger processing, the K-40 event rate is reduced by around two orders of magnitude. The L1 event rate per hDOM (31PMT) induced by K-40 is studied. We adjust two parameters of L1 trigger, coincidence photon number α and time window β . An L1 event is defined as at least α photons occur in β ns at different PMTs in one hDOM.

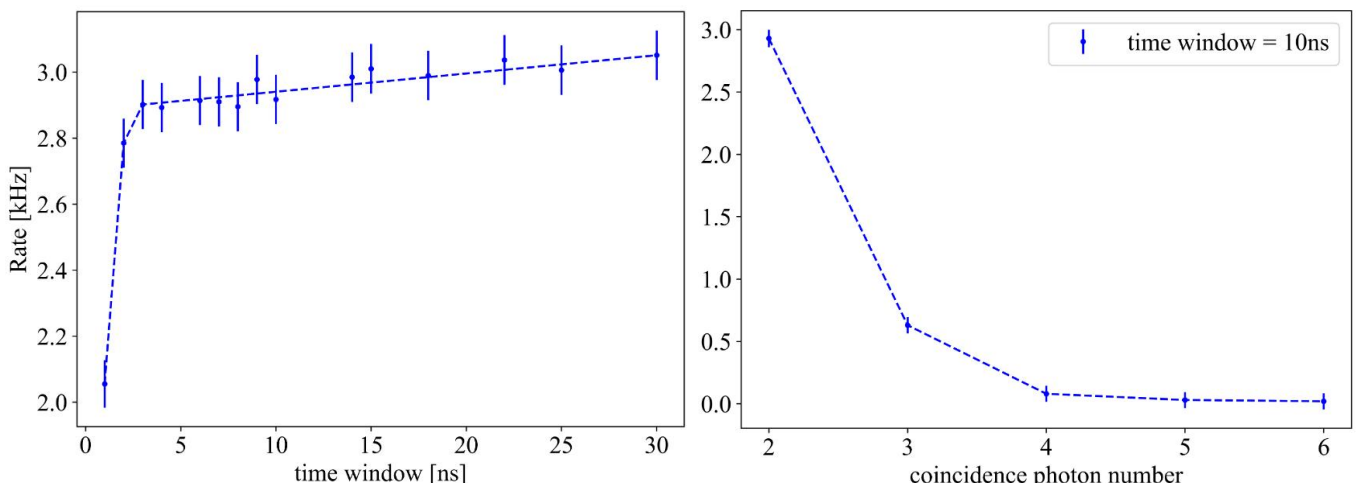


Figure 22 K-40 Trigger Rate in one hDOM.

In Figure 22, the left panel is the K-40 trigger rate changing along with the time window β . The right panel is the K-40 trigger rate decreases as the coincidence photon number α increasing. We do not require that two coincidence photons should be in different PMTs here. If do so, the rate shown above can drop around 50% additionally.

These coincidence photons mostly come from the same decay events, so the expected time interval of coincidence photon pairs is quite small in fact, as shown in Figure 23. As the time window increases, those photons which possess a larger time interval can pass the L1 trigger. So The trigger rate is gradually increasing. After the time window becomes larger than 10 ns, almost all coincidence photons

have already been involved and the trigger rate become gradually saturated.

Finally, as the time window approaches 30 ns, the trigger rate seems to converge to around 3kHz (If the different PMT condition is added, it will be around 1.5kHz). The message we can take from the trend is that after a certain value, such as 10 ns, the time window is not important for the L1 trigger. The algorithm is not sensitive to this parameter anymore.

The coincidence photon number is another parameter in the L1 trigger algorithm. It describes the threshold in the photon multiplicity. The K-40 L1 trigger rate decreases sharply as the number increases. It is intuitive to think that if the probability that one K-40 decay generates a photon that can land in the hDOM is p , then the two-photon case corresponds to p^2 and the three-photon case is p^3 . The probability p here describes mainly the absorption effect of seawater. And the number uncertainty of Cherenkov photon emission can also influence p slightly. Consider 2 photons in 10ns and 3 photons in 10ns, the former one is 2.9kHz while the later one is 0.6kHz. Increasing the photon number threshold is quite effective in L1 trigger to reduce the K-40 decay events.

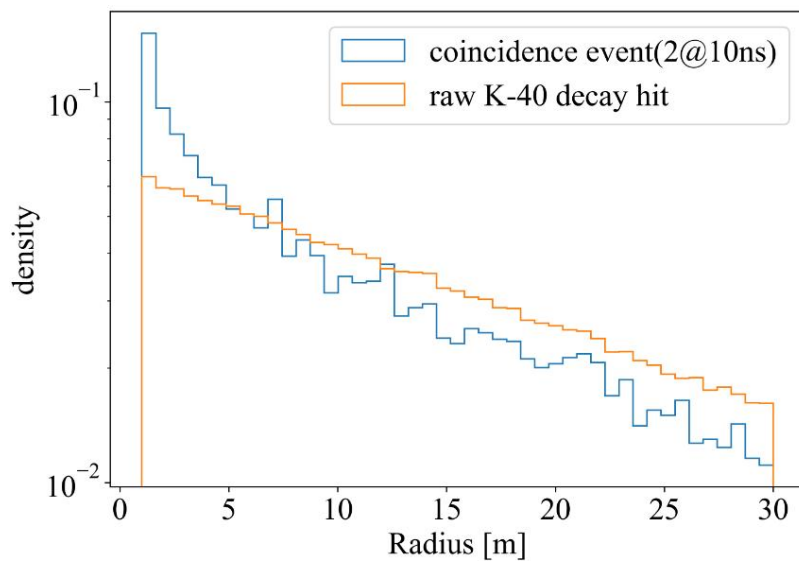
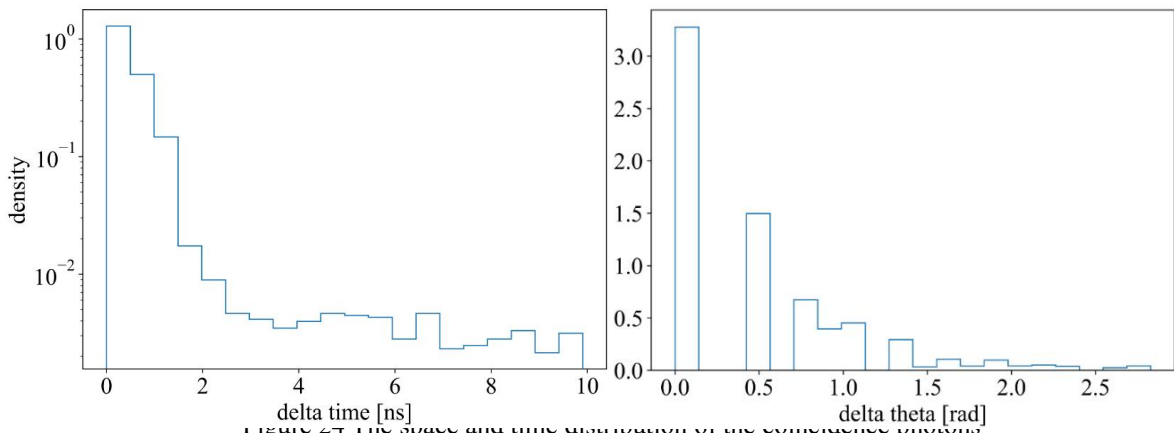


Figure 23 The radius where the detected K-40 decay events occur.

In Figure 23, the x-axis denotes the distance between K-40 events and the hDOM. We can notice that captured double coincidence events are more likely to happen near the hDOM, which leads to the fact that double coincidence is rarer than single hits. This is also a reason for our simulation to choose 30 m as the total radius of the world. Coincidence events basically only happen near the hDOM. If conducting raw hit rate analysis, a larger radius is required.



In Figure 24, the trends in the two pictures are similar. The left panel is time interval of two coincidence photons. The right panel is the angle difference of two coincidence photons on the hDOM.

As the radius increases, the volume of water space increases ($dV = 4\pi r^2 dr$). Meanwhile, the solid angle of hDOM to the K-40 events is decreasing correspondingly ($d\Omega = \frac{dA}{4\pi r^2}$). The radius factor is canceled mutually. So the trend that coincidence events are closer to hDOM in Figure 22 comes from the absorption of seawater. If the K-40 decay event is far from hDOM, then emitted photons will be largely absorbed. This absorption effect reduces the photon multiplicity, which provides the guidance of L1 trigger design.

The space and time distribution of photons from K-40 decay on the hDOM is the key factor to be considered in designing L1 trigger. The PMTs are not distributed evenly on the hDOM, while the K-40 decay events are uniformly set in space and time. In the end, all PMTs possess equal chances to capture photons all the time. The characteristic in Figure 23 shows that a coincidence pair is very likely to gather together in both space and time. 46.32% of coincidence photons fall in the same PMT. This is the reason to develop a tight version of the L1 trigger (we can reduce the 46% by regulating photons should be in different PMTs). Moreover, the time interval is quite small. This is the reason that the time window β does not matter very much in the L1 trigger (the expected time interval is 0.6ns without considering the TTS of PMT. It is still much smaller than 10ns).

Another key dimension of the trigger algorithm is the output bandwidth. We choose to read all waveforms of the PMTs and all TDC information of SiPMs. The factor that converts the Hz value to the bandwidth in MB/s is given by the expression below.

$$f_1 = 31(\text{PMTs}) * 500\text{point} * 16\text{bit}/\text{point} * (1/1021/1021/8)\#(1)$$

$$f_2 = 24(\text{SiPMs}) * 100\text{bit} * (1/1021/1021/8)\#(2)$$

f_1 and f_2 is computed from PMT and SiPM digitization methods correspondingly. After multiplying these two factors, Figure 21 will be converted to Figure 24. Bandwidth per hDOM is shown, which is almost the total output bandwidth for one hDOM.

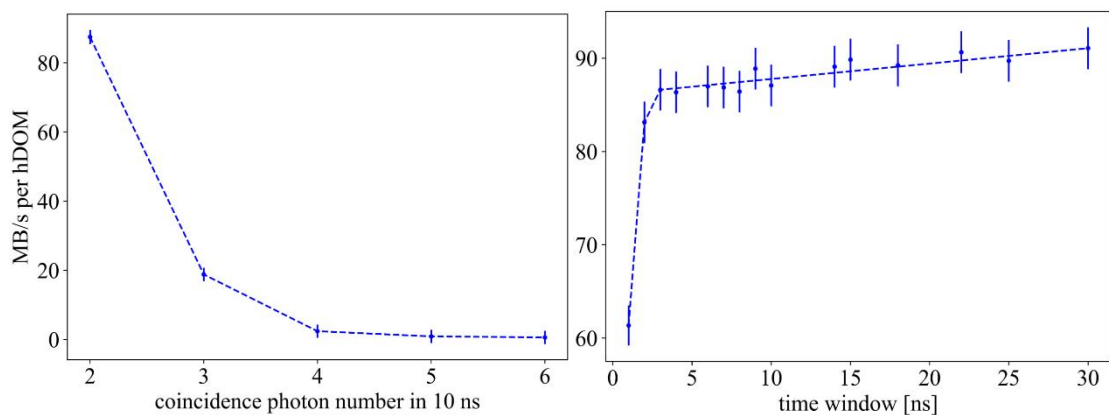


Figure 25 Bandwidth Estimation: K-40 L1 trigger rate

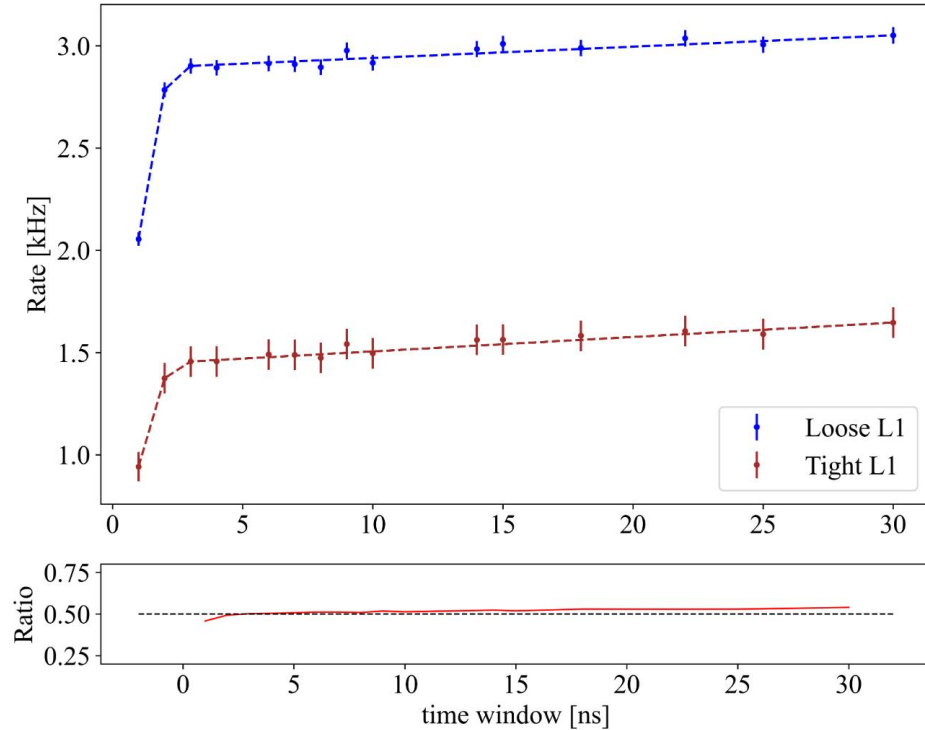


Figure 26 Comparison of Loose L1 and Tight L1 trigger.

Ratio in Figure 26 is defined as the tight trigger rate divided by the loose trigger rate. It is very close to 50% generally. This is because most double coincidence distributed in the same PMT. If we regulate that two photons should be in different PMTs, then the rate will be reduced to half.

5.3 Signal Event Evaluation

Muon events are simulated to evaluate the efficiency of L1 trigger algorithm. Muons deposit energy in water by both stochastic process and ionization. While the latter process only generates a large number of low-energy electrons, whose energy will not be recorded by hDOM. Cherenkov photons from muons as well as stochastic energy loss will be captured. Since the muon track is quite long, and the Cherenkov angle is relatively fixed, the reconstruction error is the smallest among all other neutrino reaction channels. It is the golden channel to search sources by muon for the neutrino telescope. We expect that muon events should be L1-triggered when the energy is enough or the distance is small. The results presented below are all conducted by the tight version of the L1 trigger. We demand that photons should be distributed in at least two PMTs. This shows the upper limit of the physics loss of our algorithms.

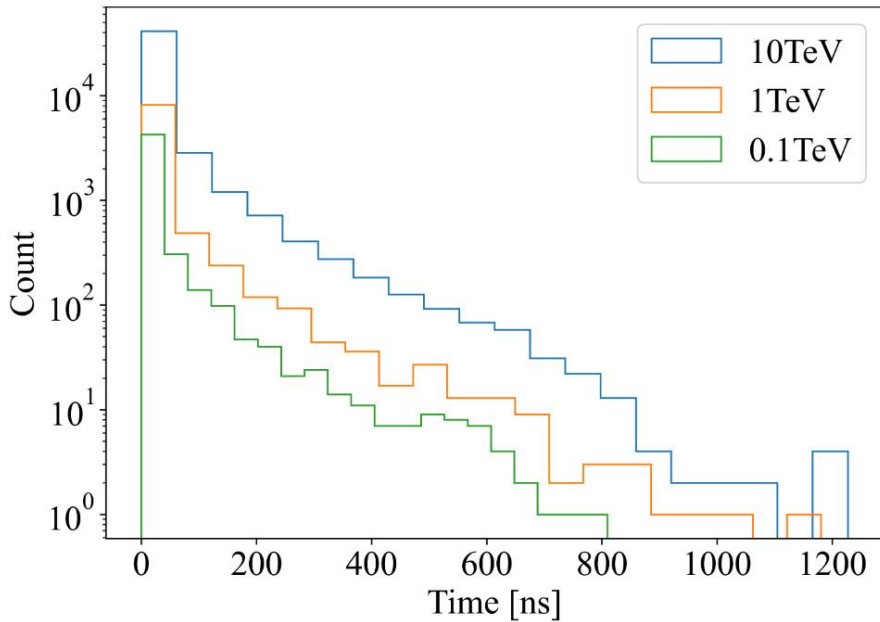


Figure 27 Stacking hit time distribution of Muon events.

In Figure 25, 1000 muon events in three kinds of energy travel through one hDOM, and the distance is fixed at 30m. The direction of muons is randomly sampled. The total number of photons is proportional to the energy as the sample number is fixed. The time distribution shows the trend of exponential decay. Most photons are limited to a short time range. The tail of time distribution is quite long. This is due to the scattering effect as well as potential stochastic energy loss. Generally, the long tail occupies quite a small percentage.

The number of photons from a muon track satisfies the following expression:

$$N(r) = \frac{N_0}{r} e^{-\frac{r}{\lambda}} \#(\mathcal{I})$$

λ here denotes the attenuation length. $\frac{1}{r}$ factor comes from the column symmetry. The rough fitting of the photon number from the simulation shows that λ is about 16.1m, close to the water optical parameter setting.

The L1 trigger ratio is calculated to mark the ability of the L1 trigger algorithm to retain muon events. This ratio is defined as

$$\text{ratio} = \frac{\text{Number of L1-triggered events at (energy, distance)}}{\text{Number of total simulation events at (energy, distance)}} \#(2)$$

When distance between the hDOM and the track is very far, or the energy is small, the ratio will be quite small. When the distance is small or the energy is large enough, we expect that the ratio can reach 100%.

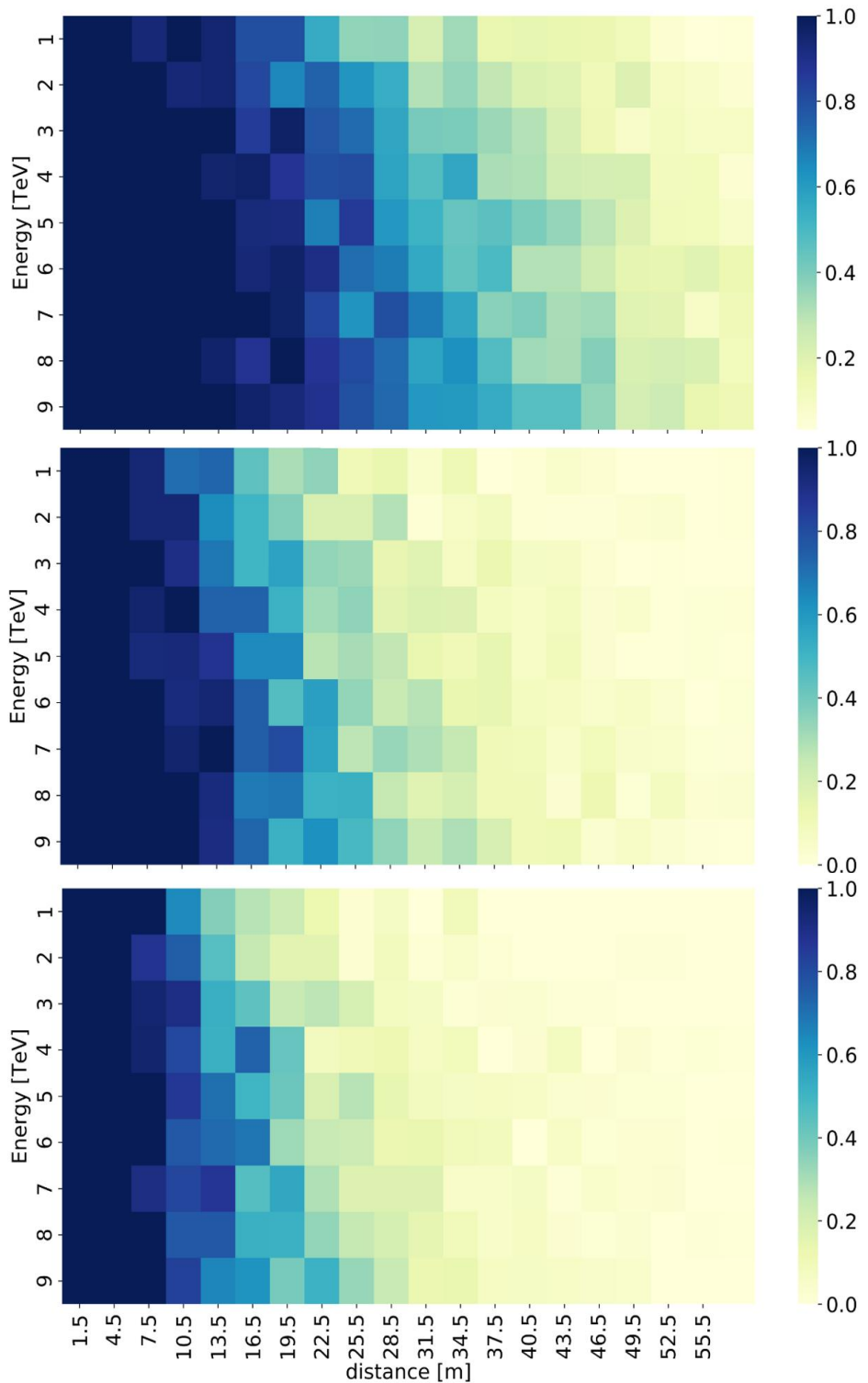


Figure 28 The L1 trigger ratio VS the energy and the distance of the muon track.

The top panel: the ratio of muons that generate hDOM photon hit and total muon set. The

middle panel: the ratio of L1 triggered muons and total muon set when $(\alpha, \beta) = (2, 10)$.

The bottom panel: the ratio of L1 triggered muons and total muon set when $(\alpha, \beta) =$

$$(3, 10)$$

The trend from the top to bottom in Figure 26 shows that blue part (more blue, higher ratio) gradually fades, as the stricter trigger criterion is applied. L1 trigger algorithm will more or less confine the muon events in the subtle region (energy is around 1TeV, distance is around 20m). In the real case, one muon track will pass through multiple hDOMs, some of them will be L1-triggered while others are not. The L2 trigger such as the cylinder method should be involved in this analysis when making decisions.

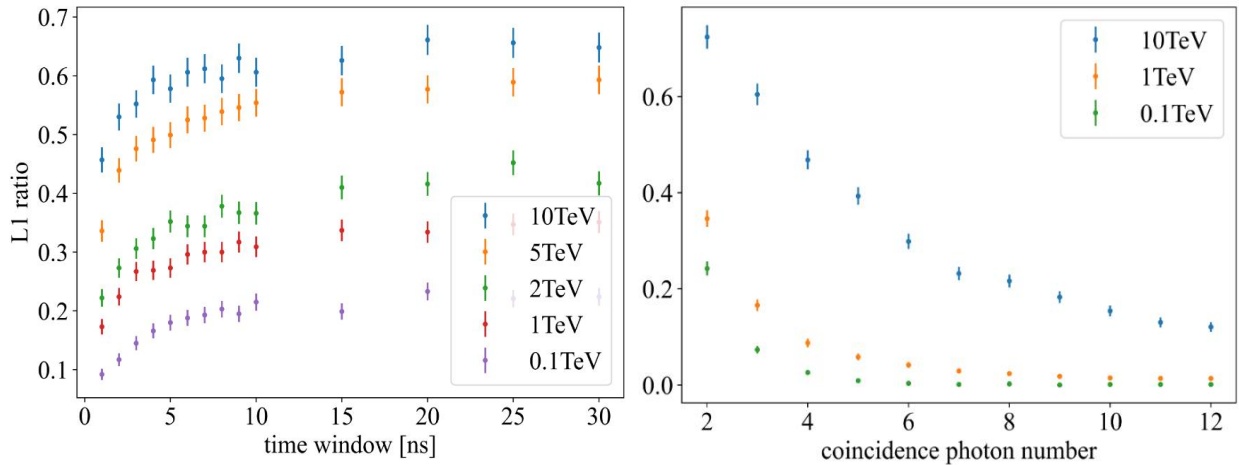


Figure 29 More precise depiction of the L1 trigger ratio.

The trend meets our expectations in the Figure 29. The left panel is the L1 trigger ratio versus the time window β . The right panel is the L1 trigger ratio versus the coincidence photon number α . The looser our L1 trigger algorithm is (larger time window and smaller coincidence photon number), the more muon events can pass the trigger. The conclusion from this figure is the same as the K-40. L1 is not sensitive to β , while stays quite sensitive to α . Because the time interval of coincidence photons from muons is quite limited. The photon multiplicity in the end is still the most important of all.

The bandwidth estimation of atmosphere muon events is around 1MB/s/hDOM. The calculation here is conducted by assuming 7kHz atmosphere muon rate and 100 photons on average for each muon. Then the bandwidth is calculated by

$$\text{bandwidth} = 7\text{kmuon} * 100/\text{muon} * (f_1 + f_2)/22420\text{hDOM} \sim 1\text{MB/s} \#(3)$$

The number might not be accurate since the rate of atmosphere muon as well as the number of photon emission strongly depends on energy. It is far from accuracy to only use one number to represent all. But the order of magnitude is not that far. The bandwidth is much smaller than K-40 ($\sim 80\text{MB/s}$).

3.3 Summary

1. dark noise

The raw dark count rate is 9000Hz for 31PMTs. After L1 trigger, this rate becomes around 1Hz. The bandwidth is negligible.

2.K-40

Reduction of K-40 strongly relies on the coincidence photon number α , instead of the time window β . If we regulate that those photons should be in different PMTs, 46.3% of coincidence events can be removed.

The bandwidth estimation is shown in Figure 24.

3.muon events

The time window β is not a very sensitive parameter, while the coincidence photon number α is. The detailed response of L1 trigger ratio with energy and distance is in Figure 26 and Figure 27.

The bandwidth of muon events is roughly on the level of 1MB/s/hDOM if ADC information of 31 PMTs and TDC information of 24 SiPMs is transmitted.

Chapter Four Future Improvements and Outlook

4.1 L1 Trigger Optimization

The L1 trigger currently has two version. The tight one requires the two photons on two different PMTs, while the loose one do not involve any requirements of PMT number. Another possible solution evolved of these is to regulate that two PMTs that is very close are hit, or two PMTs that is very far are hit, then it is an L1 trigger. The K-40 background reduction ability can be estimated by checking the right panel of Figure 23. If we use two PMTs that are far from each other to conduct L1 trigger, then the K-40 rate can decrease another one order of magnitude. While its influence on the loss of physics signals such as muon events should also be considered seriously.

It is still very difficult to decide what is the ultimate L1 trigger. The stricter our trigger criterion is, the more loss we are facing and the more background we can reduce. It seems that the decision becomes an endless trade-off. We either choose to go with less burden but more loss, to go with more weight but less missing. Maybe we should develop a reasonable way to define the signal-to-noise ratio on the one-hDOM level. Or we just consider the limit from the hardware capacity and use TDC to transmit everything to shore as a backup. After all, for the neutrino telescope aiming to observe the frontier, no loss in the first step should be bared.

There are still some unfinished pieces about the L1 trigger. The first one is that after 1000ns waveform readout, there is around 3000ns dead time of SCA-ADC. This is because the speed of digitization is around three times slower than the buffer. We still lack this part of the evaluation. Is it possible to overcome this in electronics? If not, what is the impact on the physics signals? It may not be a huge difference, since the 1000ns time window is long enough to include almost all for one hDOM. It is quite rare for hDOM to observe such long photon bursts.

The second one is what is the influence of the L1 trigger on cascade-like events. It is quite natural to find out that those hDOMs near the reaction vertex get an L1 trigger, while those far hDOMs are not. Roughly speaking, only 50% hDOMs are L1-triggered for a cascade event. The results are shown in Figure 28. Those hDOMs far from the shower, carrying limited information, are not likely to be triggered. 1000 10TeV electron neutrino char-current events are simulated.

The third one is that we should more or less evaluate the trigger algorithm by accessing higher-level information. Maybe simulate tens of thousands of events and draw the effective area plot of the detector. Different L1 & L2 trigger algorithms should not influence the effective area plot very much when the

energy is enough (for example, above 10TeV). Since this underlying trigger algorithm should not influence the event selection (say at least 10 photons on two strings) significantly, or the design of trigger is failed.

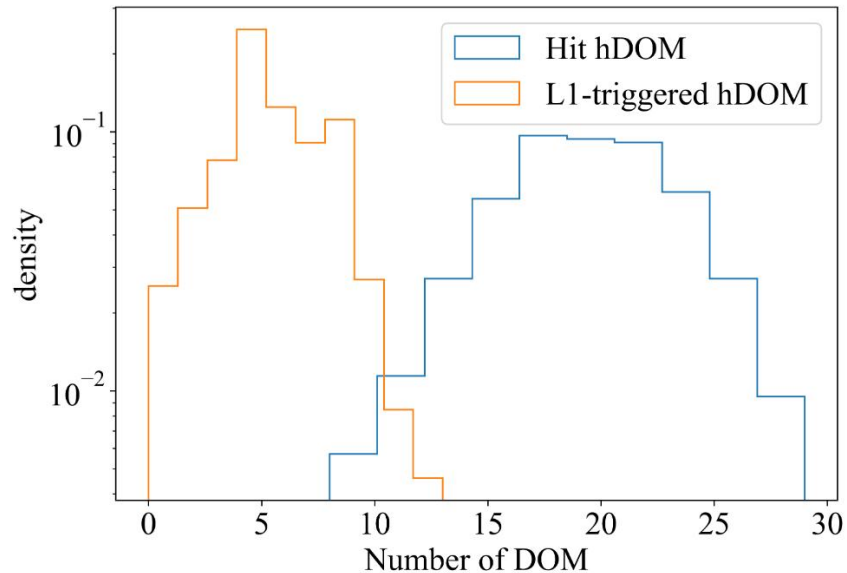


Figure 30 The number distribution of L1-triggered hDOM for an electron neutrino event.

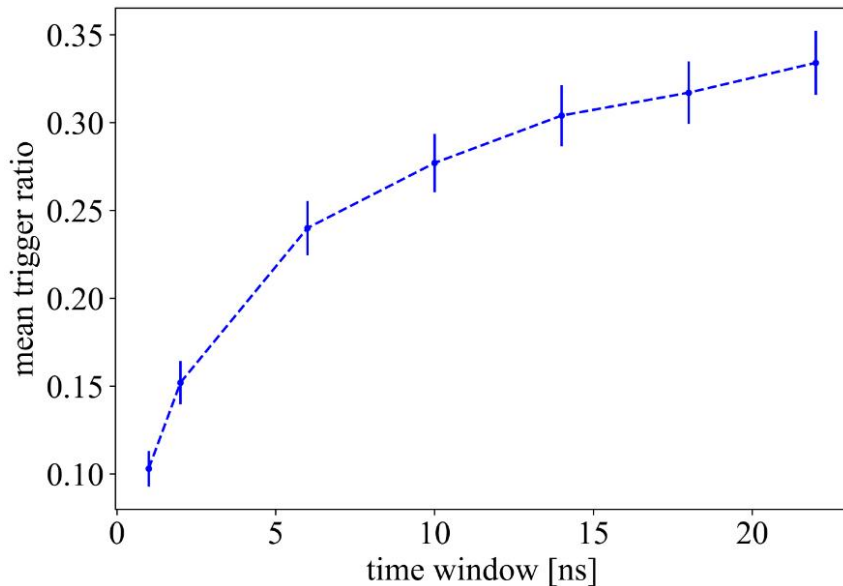


Figure 31 The mean trigger ratio VS the time window of the L1 trigger.

The ratio in Figure 31 for a cascade event is defined as the number of L1-triggered hDOMs divided by the total number of hDOMs. The curve increases slowly. After the time window is larger than 10, this ratio shows the trend of saturation. This appearance is coherent with the results from K-40 and muon events. For those hDOMs far away, only one photon is captured. It is not possible for them to pass the L1 trigger. Expansion of the time window cannot save those hDOMs.

4.2 Physics Filter Optimization

The L1 trigger places emphasis on the K-40 background reduction. This part, named as physics filter, or the L2 trigger, will focus on the extracting of physics signals. All physics purposes can generate their corresponding L2 proposals. The threshold of a certain physics event detection should be studied. The false trigger rate induced by other physics processes and the true event trigger rate should be studied for all kinds of physics filter. The work presented here is some preliminary results. More research should be conducted in the future.

4.2.3 Inter-hDOM Trigger Preliminary

If two adjacent hDOMs are both L1 triggered in a certain time window, then these two hDOMs are inter-hDOM triggered, which is an indication of potential interesting physics events. The time window should be determined by the distance between two hDOMs. In the Penrose tilt, the inter-string distance is 70m or 110m. And the distance of two adjacent hDOMs in the same string is around 20m, not fully determined yet. Since the K40 L1 trigger rate is around 1.5kHz using tight L1 trigger or 3kHz using loose L1 trigger, it is still possible that two hDOMs are triggered by K40. In seawater, photons travel around 20cm in 1ns, and high energy muons travel in vacuum light speed, which is around 30cm in 1ns. The time window for 20m should be at least 60ns.

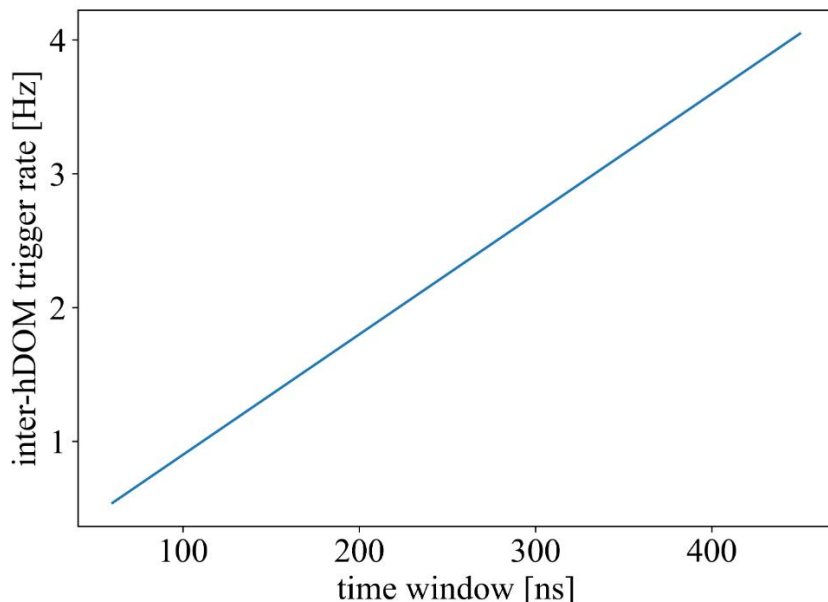


Figure 32 The inter-hDOM trigger rate VS time window

In Figure 33, we assume that the K40 L1 trigger rate is 1.5kHz. Two adjacent hDOMs are inter-hDOM triggered if they are both L1 triggered in certain time window, which is the variable in Figure 33. We use the equation implemented in 5.2 in dark noise to compute the inter-hDOM trigger rate. The

inter-hDOM trigger rate induced by K40 can be around 1Hz. For 1211 hDOMs in the whole detector, there is around 4k adjacent hDOM pairs, contributing to approximately 4kHz total inter-hDOM trigger rate.

4.2.2 Cylinder Method

If there is several nearby L1-triggered hDOMs (say $N(L1) > 3$), a pre-defined set of directions which can isotropically cover the sky are tested. The inequation (6) is tested.

A detailed description of the mathematics can be checked in (2). The idea is to extract a cylinder of hDOMs to conduct further hit selection and reconstruction. The total number of the neutrino telescope is 22420. If we only check the data from hDOMs inside a selected region, the data amount as well as the computation consumption can be significantly reduced.

In order to preliminarily test to the ability of the method to confine the direction, we select 100 muon neutrino events, the energy is from 10TeV to 10PeV. For each event, we randomly sample 500 directions. We check every direction by the inequations. If most photons can satisfy the inequation, then the direction is retained. Otherwise, it is dropped. We expect that only the directions that are close to the real injection direction can pass our test. If the direction is far from the real direction, most photons are not able to satisfy the inequation. Then they are viewed as ‘the wrong direction’.

The benefit of this method is that it is quite simple and straightforward. If there are N photons, there are $N(N - 1)/2$ relations to be checked. In fact, it is not necessary to compute all. Randomly selecting a certain part of photons can realize our goal.

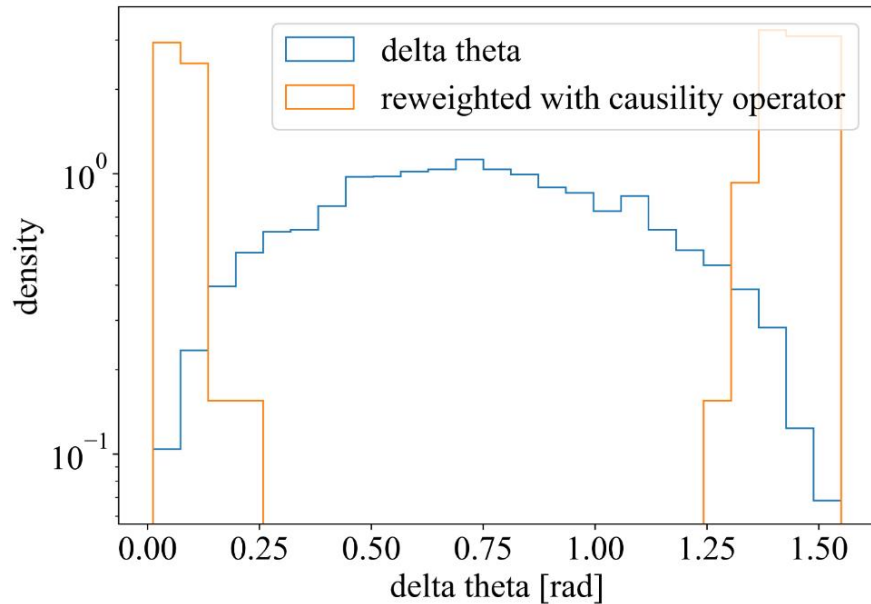


Figure 33 delta theta distribution.

Delta theta here is defined as the angle between the tested direction and the real direction. The trend is consistent with the expectation. Only the direction that lays within 0.2rad error can pass the test. This result indicates that we have the ability to select a rough cylinder region for further reconstruction.

There are a lot to be done about this in the future. The generation of noise-and-signal mixed simulation dataset, the threshold of the algorithm, the radius of the cylinder, the calculation method optimization, hit selection method after this cylinder selection, and the CPU usage estimation should be analyzed and checked in detail.

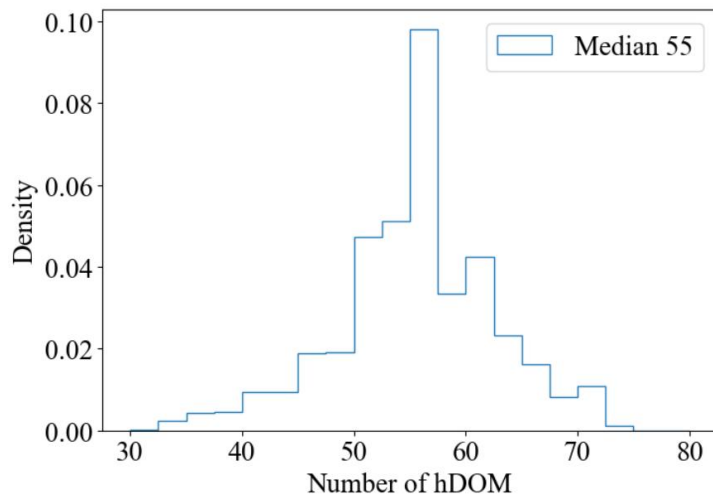


Figure 34 60000 cylinders with radius 100m are sampled to cut the Penrose tilt geometry.

In Figure 33, the cylinders are infinitely long and the number of hDOMs inside the cylinder are

recorded. The histogram shows that around 55hDOMs are inside one cylinder. Compared to 22420 hDOMs in total, this is a small number.

4.2.3 Particle Identification

This step is in fact not viewed as a part of the trigger system. After the physics filter step (L2 trigger), hit selection, particle identification, and event reconstruction should be conducted. Here, we are trying to implement a fast calculation to distinguish track-like events and cascade-like events. We define the ‘inertia tensor’ of photons.

$$I_{ik} = \begin{bmatrix} \sum m(y^2 + z^2) & -\sum mxy & -\sum mxz \\ -\sum myx & \sum m(x^2 + z^2) & -\sum myz \\ -\sum mzx & -\sum mzy & \sum m(x^2 + y^2) \end{bmatrix}_{\#} \quad (1)$$

The parameter ‘m’ in fact is the charge. The x,y, and z is the coordinates of the photon hit.

We use the value T to evaluate the shape of the photons. T is defined as

$$T = \frac{I_{max} - I_{min}}{I_{max} + I_{min}} \#(2)$$

I_{max} and I_{min} is the maximum eigenvalue and the minimum eigenvalue of the inertia tensor. For a perfect sphere, T is zero. And for a ideal thin stick, T is zero.

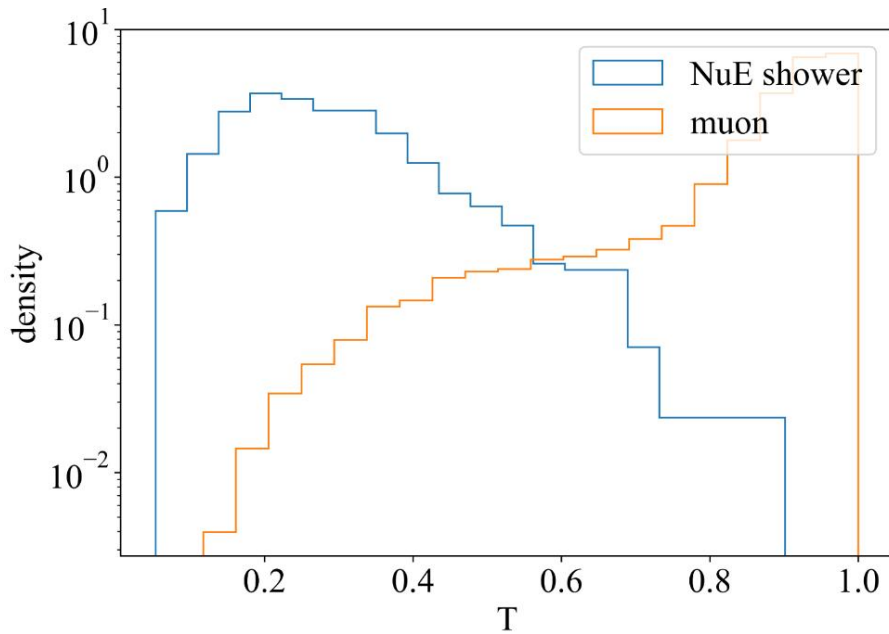


Figure 35 The T value distribution for both track-like events and cascade-like events.

In Figure 34, 29000 NuE events and 1000 muon events are simulated. Actually, two distributions are

overlapped a little bit, which indicates there should be a threshold. In the future, more statistics magnitude should be involved. And energy and time dimensions should be considered and analyzed.

4.3 Non-loss Compression Method on Waveform

Currently, electronics can clip the baseline of a waveform to reduce the total bandwidth of one hDOM.[38] Normally, a piece of the waveform is generally not always rising or falling, they are mostly fluctuating with baseline. The waveform in Figure 36 is from a dark noise single photon event. If the baseline part is abandoned, the total bandwidth can be reduced.



Figure 36 Example of a three-inch PMT.

We conduct a simple waveform simulation. The input of the simulation is a discrete time series of photon hit, such as the time column of Geant4 output. The output of the simulation is the waveform, just like the readout from ADC.

The template of the single-photon waveform is analytically expressed as

$$V = A \cdot t e^{-\frac{t}{\lambda}} \#(1)$$

A is proportional to the peak value of the waveform. In fact, the peak value is $A\lambda e^{-1}$. Let the start point be 0, then the waveform will reach the peak in $t = \lambda$. Because this numerical model only possesses one degree of freedom, it is quite straightforward that both the rising time and the falling time are proportional to λ . When the waveform is stable, this can be a good approximation.

To mimic a real case, more components of the waveform should be considered in the simulation.

1. Baseline Fluctuation: normally use a Gaussian distribution with sigma equal to ~ 0.1 mV to sample

this fluctuation

2. After Pulse (AP): The delay time distribution and the pulse charge should be regulated.
3. Transient Time Spread (TTS): The smearing effect of the photon hit time. Normally, we add a Gaussian distribution to the input time list. The sigma of the Gaussian is 50ps for 1-inch PMT and 0.6ns for 3-inch PMT.
4. Dark Count (DC): The rate of dark noise should be regulated. The number of dark photons is sampled using the Poisson Distribution. Then the uniform distribution will be implemented to sample the time of dark noise.
5. The shape of Waveform: The numerical model can be used as a default. It is also a choice to average the real PMT data to get this template. In Figure 37, the time granularity of 1ns is assumed.

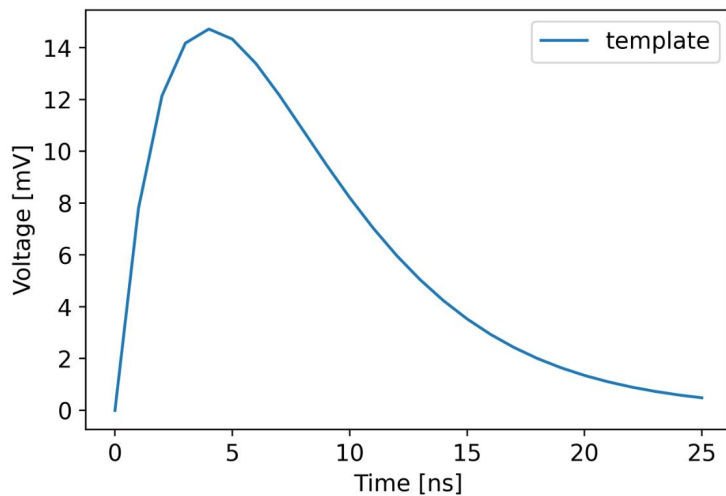


Figure 37 Template of a single-photon waveform. $A = 10$ and $\lambda = 4$ are assumed.

The waveform technique can be a new method to recognize double pulse signals from tau neutrino[39][40], which can be a potential breakthrough in the neutrino telescope in the future. In this chapter, we focus on the ratio of the baseline part in the waveform to the signal part. The question we are trying to answer is how much bandwidth from the waveform digitization we can reduce by clipping the baseline.

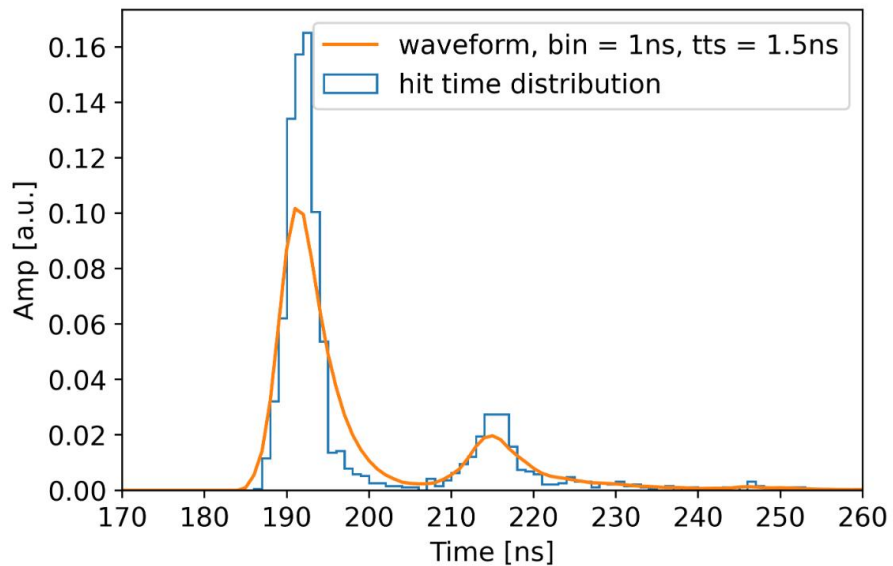


Figure 38 An example of waveform simulation. The baseline fluctuation is not added here.

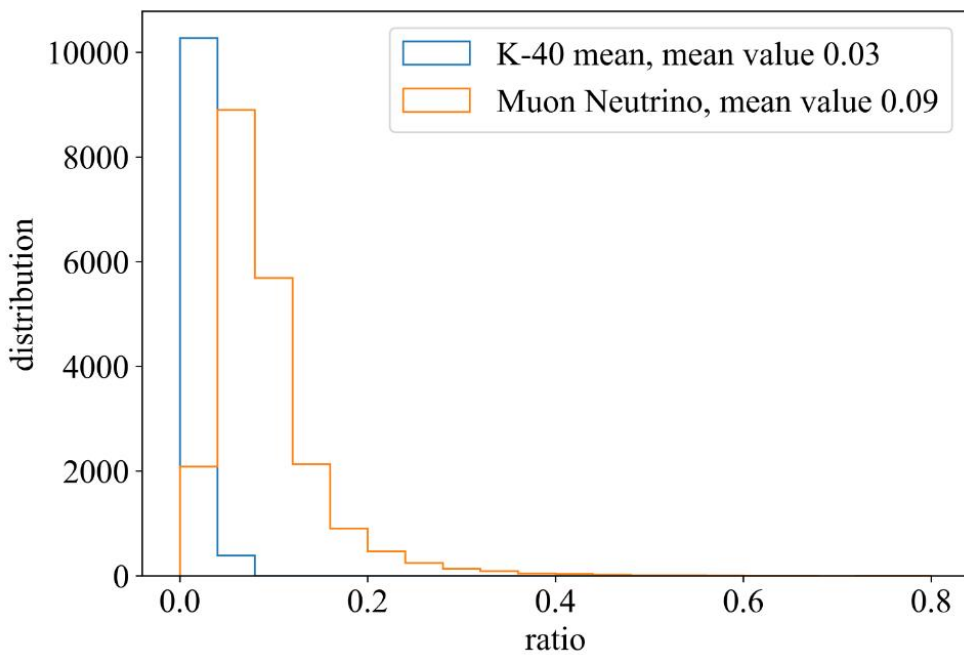


Figure 39 The signal ratio distribution

In Figure 39, we use the output from K-40 simulation and muon neutrino simulation as an input to generate 10000 waveform pieces by the waveform simulation. In each waveform pieces, 500 points with 2ns time interval are assumed. The baseline fluctuation is not added. The ratio is defined as the number of points with signals divided by 500. In general, the ratio is around 5%. This indicates that 95% bandwidth can be reduced by the baseline clipping technique in the hDOM.

4.4 Conclusion

In the first chapter, we discuss the general characteristic of signal band background of TRIDENT, which leads to the necessity and feasibility of the trigger system. We consider utilizing the correlation feature in the signal to extract physics events and reduce the bandwidth. Moreover, we first present the basic information of the trigger algorithm for other neutrino telescopes in the first chapter. The trigger information of KM3NeT and IceCube are presented in detail to provide reference for our research. In the second chapter, we present a preliminary skeleton design of the trigger system. Two parts, L1 Trigger and L2 Trigger, constitute all trigger strategy. The L1 trigger is discussed in detail, including the general hardware implementation framework. In the chapter three, we construct a simulation pipeline to evaluate the performance of the L1 trigger in detail, including its ability to reduce the dark noise as well as its influence on the muon events. In the end, we provide the optimization guidance for the L1 trigger and some conceptual demonstrations of the L2 trigger are discussed. Baseline clipping technique is also discussed and evaluated as another idea to reduce the bandwidth, in which some simple waveform simulations is introduced as supplementary instruction.

References

- [1] Enz C P . 50 years ago Pauli invented the neutrino[M]. 1982.
- [2] Wang, K. A Suggestion on the Detection of the Neutrino. Physical Review, 61, 97-97. 1942
- [3] Cowan C L , Reines F , Harrison F B , et al. Detection of the Free Neutrino: a Confirmation[J]. The Theory of Beta-Decay, 1969, 122(14):129-135.
- [4] Gonzalez-Garcia M C , Maltoni M . Phenomenology with Massive Neutrinos[J]. Physics Reports, 460.
- [5] Avignone Iii F T , Elliott S R , Engel J . Double Beta Decay, Majorana Neutrinos, and Neutrino Mass[J]. Review of Modern Physics, 2007.
- [6] Gaisser T K , Engel R , Resconi E . Cosmic rays and particle physics[J]. Cosmic Rays and Particle Physics
- [7] Aartsen M G , Abbasi R , Abdou Y , et al. Evidence for High-Energy Extraterrestrial Neutrinos at the IceCube Detector[J]. Science, 2013, 342(6161):1242856.
- [8] Aartsen M G , Ackermann M , Adams J , et al. Multimessenger observations of a flaring blazar coincident with high-energy neutrino IceCube-170922A. 2018.
- [9] Collaboration I C , Abbasi R U . Search for muon neutrinos from Gamma-Ray Bursts with the IceCube neutrino telescope:, 10.1088/0004-637X/710/1/346[P]. 2009.
- [10] Abbasi, R. et al. (2022g). Search for neutrino emission from cores of active galactic nuclei. Phys. Rev. D, 106(2):022005.
- [11] The contribution of Fermi-2LAC blazars to the diffuse TeV-PeV neutrino flux[J]. Astrophysical Journal, 2016, 835(1):45.
- [12] Constraints on Galactic Neutrino Emission with Seven Years of IceCube Data[J]. Astrophysical Journal, 2017, 849(1):67.
- [13] Collaboration I C , Aartsen M G , Ackermann M , et al. A Search for Neutrino Emission from Fast Radio Bursts with Six Years of IceCube Data[J]. 2017.
- [14] Multi-messenger Observations of a Binary Neutron Star Merger[J]. The Astrophysical Journal, 2017, 848.
- [15] Toscani M . Tidal disruption events in the multi-messenger astronomy era[J]. Il Nuovo Cimento della Societa Italiana di Fisica, C. Geophysics and space physics, 2021(2/3):44.

- [16] Markov, M. A. "On high-energy neutrino physics". In Sudarshan, E. C. G.; Tinlot, J. H.; Melissinos, A. C. (eds.). Proceedings of the 1960 Annual International Conference on High-Energy Physics. University of Rochester. p. 578.
- [17] O, Kavatsyuk, Q, et al. Multi-PMT optical module for the KM3NeT neutrino telescope[J]. Nuclear Instruments & Methods in Physics Research, 2012.
- [18] Collaboration I C . The IceCube Data Acquisition System: Signal Capture, Digitization, and Timestamping[J]. 2008.
- [19] company, H. Photomultiplier Tubes: Basics and Applications. Hamamatsu company, 2017, 3 edition.
- [20] Fa A , Sgb C . Understanding and simulating SiPMs[J]. Nuclear Instruments and Methods in Physics Research Section A: Accelerators, Spectrometers, Detectors and Associated Equipment, 2019, 926:16-35.
- [21] The Giant Radio Array for Neutrino Detection(GRAND):Science and design[J]. Science China(Physics,Mechanics & Astronomy), 2020, v.63(01):5-47.
- [22] Collaboration I C , Aartsen M G , Ackermann M , et al. The IceCube Neutrino Observatory: Instrumentation and Online Systems[J]. Journal of Instrumentation, 2016, arXiv:1612.05093 [astro-ph.IM](3).
- [23] S Adrián-Martínez, Ageron M , Aharonian F , et al. Letter of intent for KM3NeT 2.0[J]. 2020.
- [24] Resconi E , Collaboration P O . The Pacific Ocean Neutrino Experiment[J]. arXiv e-prints, 2021.
- [25] Stasielak J , Malecki P , Naumov D , et al. High-Energy Neutrino Astronomy—Baikal-GVD Neutrino Telescope in Lake Baikal[J]. Symmetry, 2021, 13(3):377.
- [26] Ye, Z. P., et al. Proposal for a neutrino telescope in South China Sea. arXiv preprint arXiv:2207.04519, 2022.
- [27] Fan Hu, Zhuo Li, and Donglian Xu. Exploring a PMT+ SiPM hybrid optical module for next generation neutrino telescopes. arXiv preprint arXiv:2108.05515, 2021.
- [28] Aartsen M G , Abbasi R , Ackermann M , et al. IceCube-Gen2: the window to the extreme Universe[J]. Journal of Physics G Nuclear and Particle Physics, 2021, 48(6):060501.
- [29] Fan Hu, Optimizing the Next Generation Deep Sea Neutrino Telescope[D], Beijing: Peking University, 2023
- [30] Deep-Sea Bioluminescence Blooms after Dense Water Formation at the Ocean Surface[J]. PLoS ONE, 2013, 8(7):e67523.

- [31] T.A. Wang, C. Guo, et.al. Characterization of two SiPM arrays from Hamamatsu and Onsemi for liquid argon detector, arXiv:2210.15970v1 [physics.ins-det], 2022.
- [32] Kelley J L , Collaboration I C . Event triggering in the IceCube data acquisition system[C]// Applications of Mathematics in Engineering & Economics. American Institute of Physics, 2014.
- [33] Ronald Bruijn, Tommaso Chiarusi, et al KM3NeT Data Acquisition and and Trigger System, 2019
- [34] Herold B . Study of 40K-induced rates for a KM3NeT design option with multi-PMT optical modules[J]. Nuclear Instruments and Methods in Physics Research Section A: Accelerators, Spectrometers, Detectors and Associated Equipment, 2011.
- [35] Pellegrino C . The Trigger and Data Acquisition System (TriDAS) of the KM3NeT experiment[J]. Il Nuovo Cimento della Societa Italiana di Fisica, C. Geophysics and space physics, 2016, 39(1).
- [36] Sio, C.D.. Event triggering and deep learning for particle identification in KM3NeT.2018
- [37] Avrorin A V , Avrorin A D , Ainutdinov V M , et al. Data acquisition system of the NT1000 Baikal neutrino telescope[J]. Instruments and Experimental Techniques, 2014.
- [38] Patauner C . Lossy and lossless data compression of data from high energy physics experiments. 2012.
- [39] Xu D . Search for Astrophysical Tau Neutrinos with IceCube[J]. arXiv, 2017.
- [40] Williams D , Zarzhitsky P , Xu D . Detecting Tau Neutrinos in IceCube with Double Pulses. 2016.

Symbols and Marks Appendix 1

Research Projects and Publications during Undergraduate Period

[1]

Acknowledgements

I would like to express my sincere appreciation to Prof. Xu and everyone in TRIDENT collaboration. Their insight and expertise contribute a lot in the completion of the paper. Their constant support helps me to tide over difficulties. Those days and nights we fight together is the most precious treasure on my academic journey.

I would also like to thank my family and friends for their accompany. They give me courage to persevere the motivation through those time of confusion and pain. Without them, this work would not have been possible.

